Technology

Cell Stem Cell

# Prevention of transgene silencing during human pluripotent stem cell differentiation

## Graphical abstract

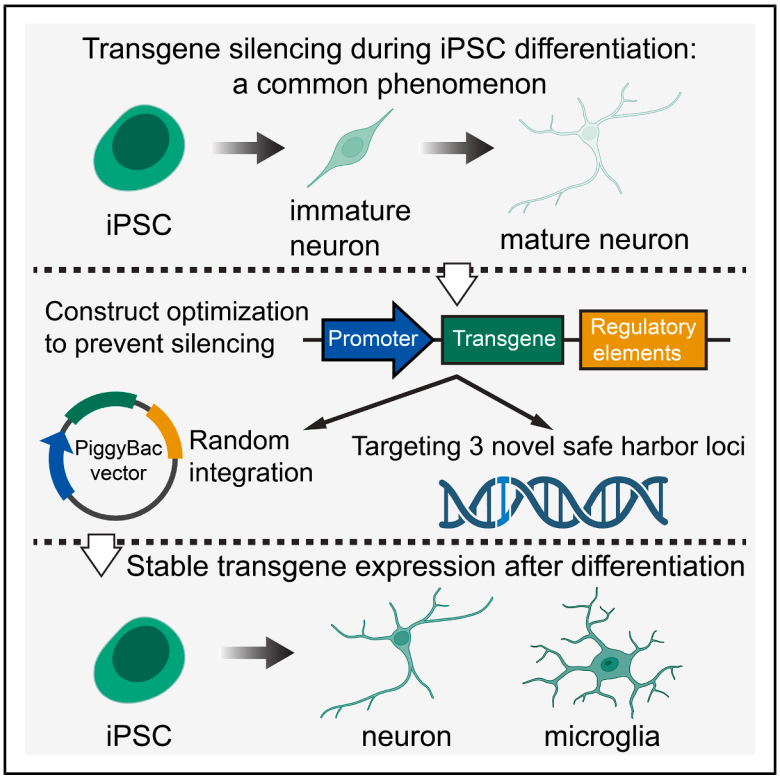


## Authors

Takeshi Uenaka, Alan Napole, Aninda Dibya Saha, ..., William C. Skarnes, Michael E. Ward, Marius Wernig

## Correspondence

wernig@stanford.edu

## In brief

Stable transgene expression remains challenging during human pluripotent stem cell differentiation. Wernig and colleagues show that combining CAG/Ubc promoters with WPRE prevents transgene silencing following both random and targeted integration. This work provides a broadly applicable genetic tool for studies requiring sustained transgene expression during differentiation of pluripotent stem cells.

## Highlights

- Transgenes are frequently silenced during pluripotent stem cell differentiation
- CAG/Ubc promoters combined with WPRE prevent transgene silencing during differentiation
- Novel safe harbor integration sites support prevention of transgene silencing
- Robust transgene expression along neuronal and microglial differentiation protocols

Uenaka et al., 2026, Cell Stem Cell *33*, 517–530
March 5, 2026 
https://doi.org/10.1016/j.stem.2026.01.007

CellPress

Cell Stem Cell

CellPress
OPEN ACCESS

Technology

# Prevention of transgene silencing during human pluripotent stem cell differentiation

Takeshi Uenaka,[1,2,3,21] Alan Napole,[1,2,21] Aninda Dibya Saha,[1,2] Duo Sun,[1,2,4] Angelina Singavarapu,[1,2] Elizabeth Calzada,[5] Jiahui Chen,[6] Lena Erlebach,[7] Amanda McQuade,[8] Daniel M. Ramos,[5] Alessandra Rigamonti,[9] Lisa Salazar,[10] Avi J. Samelson,[8] Kamilla Sedov,[2] Natalie J. Welsh,[9] Katleen Wild,[7] Qianxin Wu,[11] Ernest Arenas,[9,12] Andrew R. Bassett,[11,12] Martin Kampmann,[8,13,14] Deborah Kronenberg-Versteeg,[7,12] Florian T. Merkle,[6,12,15,16] Birgitt Schüle,[2,12] Leslie M. Thompson,[10,12,17,18] William C. Skarnes,[12,19] Michael E. Ward,[5,12] and Marius Wernig[1,2,12,20,22,*]

[1]Institute for Stem Cell Biology & Regenerative Medicine, Stanford University School of Medicine, Stanford, CA 94305, USA
[2]Department of Pathology, Stanford University School of Medicine, Stanford, CA 94305, USA
[3]The Phil & Penny Knight Initiative for Brain Resilience at the Wu Tsai Neurosciences Institute, Stanford University, Stanford, CA 94305, USA
[4]Department of Chemical Engineering, Stanford University, Stanford, CA 94305, USA
[5]National Institute of Neurological Disorders and Stroke, NIH, Bethesda, MD 20892, USA
[6]Institute of Metabolic Science, University of Cambridge, Cambridge CB2 0QQ, UK
[7]German Center for Neurodegenerative Diseases (DZNE) Tübingen, and Hertie Institute for Clinical Brain Research, Department of Cellular Neurology, University of Tübingen, 72076 Tübingen, Germany
[8]Institute for Neurodegenerative Diseases, University of California, San Francisco, San Francisco, CA 94158, USA
[9]Division of Molecular Neurobiology, Department of Medical Biochemistry and Biophysics, Karolinska Institutet, Stockholm 17177, Sweden
[10]Sue and Bill Gross Stem Cell Research Center, University of California, Irvine, Irvine, CA 92697, USA
[11]Wellcome Sanger Institute, Wellcome Genome Campus, Hinxton, Cambridge CB10 1SA, UK
[12]The Chan Zuckerberg Initiative iPSC working group, Redwood City, CA, USA
[13]Department of Biochemistry and Biophysics, University of California, San Francisco, San Francisco, CA 94158, USA
[14]The Chan Zuckerberg Initiative CRISPR working group, Redwood City, CA, USA
[15]Department of Pharmacology, University of Cambridge, Cambridge CB2 1PD, UK
[16]Cambridge Stem Cell Institute, University of Cambridge, Cambridge CB2 0AW, UK
[17]Department of Psychiatry & Human Behavior, University of California, Irvine, Irvine, CA 92697, USA
[18]Department of Neurobiology and Behavior, University of California, Irvine, Irvine, CA 92697, USA
[19]The Jackson Laboratory for Genomic Medicine, Farmington, CT 06032, USA
[20]Department of Chemical and Systems Biology, Stanford University School of Medicine, Stanford, CA 94305, USA
[21]These authors contributed equally
[22]Lead contact
*Correspondence: wernig@stanford.edu
https://doi.org/10.1016/j.stem.2026.01.007

## SUMMARY

Transgenes are often silenced upon differentiation of pluripotent stem cells using conventional expression systems. Here, we developed the TK4 PiggyBac vector to conduct a comparative analysis to evaluate the impact of various promoters, transcriptional regulatory elements, insulators, and genomic integration sites on transgene silencing during neuronal differentiation. Our findings reveal that specific combinations of CAG and Ubc promoters with the Woodchuck hepatitis virus post-transcriptional regulatory element (WPRE) can prevent transgene silencing during differentiation, whereas chromatin insulators have less impact on sustained expression. Three novel safe harbor loci, distant from known genes, as well as the citrate lyase beta-like (*CLYBL*) locus, similarly support the prevention of transgene silencing. Remarkably, the TK4 vector showed complete resistance to silencing across various neuronal and microglial differentiation protocols, as independently confirmed by seven laboratories. This construct will be highly useful for assays requiring stable transgene expression during differentiation and holds potential for broad applications in various research fields.

## INTRODUCTION

Differentiating human embryonic stem (ES) or induced pluripotent stem (iPS) cells into various cell types is an essential technology for studying human development, disease mechanisms, and potential therapeutic applications.[1] Achieving these goals often involves engineering stem cells by overexpressing transgenes or downregulating endogenous genes, which are indispensable techniques. However, a significant challenge for the field is that these transgenes are frequently silenced. This silencing occurs

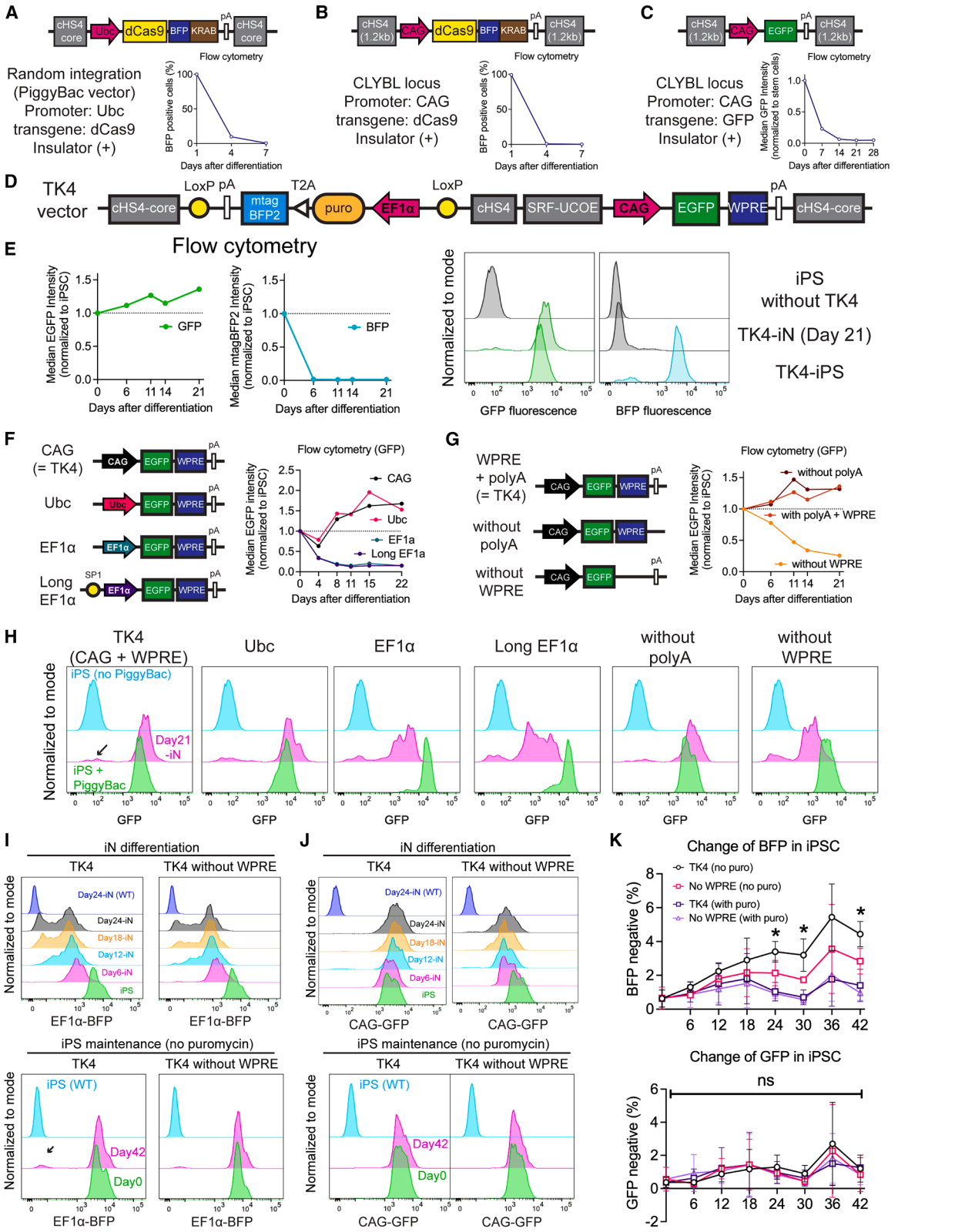


*(legend on next page)*

in both undifferentiated stem cells[2] and cells undergoing differentiation into other cell types, including cardiomyocytes,[3] endothelium,[4] myeloid cells,[5] and neurons.[6]

Several papers have reported mechanisms contributing to transgene silencing. First, specific sequences within the vector, such as long terminal repeats (LTRs) in retroviral vectors,[7] promoters,[8] or intron-less transgenes via human silencing hub (HUSH) complex,[9] can recruit DNA modifications such as DNA methylation or histone deacetylation to silence genes.[10,11] Second, integration of the vector into heterochromatin regions can lead to spreading of transcriptionally repressive epigenetic modifications.[12,13] Third, post-transcriptional mechanisms involving double-stranded RNA have been described in particular in plant and fungal cells.[14] Incorporating insulator elements into the expression vector[2,15] or targeting expression cassettes into commonly used safe harbor loci such as the adeno-associated virus integration site 1 (AAVS1)[16] or citrate lyase beta-like (CLYBL)[17] locus allowed more stable gene expression over time in proliferating, undifferentiated pluripotent stem cells. However, epigenetic marks are known to be tissue-specific,[18] and high and stable gene expression in pluripotent cells accomplished by insulators or gene targeting does not translate to sustained expression during lineage differentiation (Figures 1A–1C).

The inability to maintain exogenous gene expression throughout differentiation poses a significant obstacle for many experimental approaches, including cell labeling with fluorescent reporters and overexpressing functional proteins like disease mutant proteins,[19] genetically encoded calcium indicator modified for phototransduction (GCaMP),[20] and dead Cas9 (dCas9).[21] Most critically, this silencing issue compromises the robustness of CRISPR-Cas9-related genetic screens, which would otherwise be ideally suited for use with pluripotent stem cell platforms. Therefore, there is an urgent need to overcome transgene silencing that occurs during differentiation.

Here, we present the PiggyBac construct TK4 that can prevent transgene silencing during the differentiation of human pluripotent stem cells into neurons or microglia. Through systematic comparison, we identify a combination of transcriptional elements that effectively overcomes silencing during differentiation.

## DESIGN

A critical bottleneck in the field is the pronounced silencing of experimental transgenes during human pluripotent stem cell differentiation. To overcome this limitation, we took a two-pronged approach: (1) to test several relevant regulatory DNA elements in expression vectors and (2) to identify an optimal genomic integration site. Both approaches are known to affect gene expression, but a systematic evaluation of combinations of regulatory elements and a comparison of different genomic integration sites have not been performed yet for differentiation of pluripotent stem cells.

## RESULTS

### Establishment of the TK4 PiggyBac vector that can prevent transgene silencing during neuronal differentiation

When human pluripotent stem cells are differentiated into neurons, transgene expression is substantially silenced, either when expressed from random integrations or from defined genomic sites such as the CLYBL locus together with insulators (Figures 1A–1C). To identify an expression system that may avoid silencing, we empirically designed a multi-element PiggyBac vector (TK4 vector; Figure 1D). This vector is highly

**Figure 1. Promoter and WPRE sequences are the key elements in the TK4 PiggyBac vector that prevent silencing**

(A and B) dCas9-BFP-Krüppel-associated box domain (KRAB) was integrated into human ES or iPS cells either randomly via a PiggyBac construct or specifically into the CLYBL locus by homologous recombination using transcription activator-like effector nuclease (TALEN). The percentage of BFP-positive cells was monitored over time following neuronal differentiation; $n = 1$ for each.

(C) EGFP was integrated into the CLYBL locus by gene targeting using CRISPR, and the median EGFP intensity was measured over time following differentiation of ES cells into neurons; $n = 1$.

(D) Outline of the TK4 PiggyBac vector.

(E) EGFP and BFP fluorescence in TK4 vector-integrated iPS cells was assessed during neuronal differentiation by flow cytometry at indicated time points.

(F) Four different promoters were tested in the TK4 vector by measuring EGFP intensity during neuronal differentiation; $n = 1$. Biological replicates did not match most time points and are thus shown separately in Figure S1C.

(G) The contribution of the pA signal and the WPRE element to silencing was assessed by EGFP fluorescence intensity during neuronal differentiation by flow cytometry as indicated. The experiments for (E), (G), and (Figure S1C) were done in parallel. For convenience, we have re-plotted the EGFP line from (E) as "poly(A) + WPRE" in (G) and "CAG" in (Figure S1C); $n = 1$. Biological replicates performed with different time points are shown in Figure S1F.

(H) Representative GFP histograms from lines with different promoters or with/without poly(A)/WPRE. (Bottom) iPS cells with PiggyBac vector. (Middle) 3-week neurons with PiggyBac vector. (Top) iPS cells without PiggyBac vector (negative control). Arrow indicates the GFP-negative population in 3-week neurons containing non-labeled mouse glia.

(I) (Top) Representative BFP histograms for the TK4 vector with (left) or without WPRE (right) during neuronal differentiation. (Bottom) Representative BFP histograms for the TK4 vector with (left) or without WPRE (right) during iPS cell maintenance. Arrow indicates the BFP-negative population observed in iPS cells maintained 42 days without antibiotics.

(J) (Top) Representative GFP histograms for the TK4 vector with (left) or without WPRE (right) during neuronal differentiation. (Bottom) Representative GFP histograms for the TK4 vector with (left) or without WPRE (right) during iPS cell maintenance.

(K) (Top) BFP-negative population tracked during iPS cell maintenance for 42 days in lines containing the TK4 vector with or without WPRE and with or without puromycin. Significant differences were observed between TK4 (+puro) vs. TK4 (−puro) and TK4 without WPRE (+puro) vs. TK4 (−puro) at D24; TK4 without WPRE (+puro) vs. TK4 without WPRE (−puro) at day 30; and TK4 (+puro) vs. TK4 (−puro) and TK4 without WPRE (+puro) vs. TK4 (−puro) at day 42. $^*p < 0.05$; two-way ANOVA with Tukey's multiple comparisons test; $n = 3$. (Bottom) GFP-negative population tracked during iPS cell maintenance for 42 days in lines containing the TK4 vector with or without WPRE and with or without puromycin. No significant differences were observed. Statistical analysis was performed using two-way ANOVA; $n = 3$. Data are shown as mean ± SD.

See also Figure S1.

modular, as all elements of the transcriptional expression cassette are flanked by unique restriction enzymes that allow facile element exchange. To quantify the degree of transcriptional silencing, we introduced a cytomegalovirus (CMV) early enhancer/chicken β-actin promoter (CAG)-enhanced green fluorescent protein (EGFP)-Woodchuck hepatitis virus post-transcriptional regulatory element (WPRE)-polyadenylation (pA) expression cassette in one direction. We had previously determined that EGFP can be reliably used to measure silencing (Figure 1C). In the opposite direction, we introduced an elongation factor 1 alpha (EF1α)-puro-Thosea asigna virus 2A (T2A)-Monomeric Tag blue fluorescent protein 2 (mTagBFP2)-pA construct for drug selection of cells with successful vector integration. Upstream of the EGFP expression cassette, we further introduced the long chicken hypersensitive site 4 (cHS4)[15] and the SRF-ubiquitous chromatin opening element (UCOE) insulator elements.[22] In addition, we kept the two core regions of the cHS4 insulator element that were already contained in the original vector and flanked the entire inserted DNA cassette.

First, we integrated this TK4 vector by co-transfection with transposase into KOLF2.1 iPS cells that already contained a neurogenin 2 (NGN2)-inducible cassette.[23] Following puromycin selection, cells were passaged 5–10 times before initiating differentiation. Neuronal differentiation was induced by the addition of doxycycline in the absence of puromycin. After another 5 days, we added primary mouse glia to support neuronal maturation. We then measured the EGFP fluorescence in neurons over time by flow cytometry. Since mTagBFP2 happened to be fused to our puromycin selection cassette, we also recorded mTagBFP2 fluorescence together with EGFP (Figures S1A and S1B). As expected, mTagBFP2 expression was rapidly reduced and barely detectable after 1 week of differentiation compared with undifferentiated iPS cells (Figure 1E). Surprisingly, however, the EGFP fluorescence intensity did not decline over time. Instead, it rather slightly increased over time (Figure 1E).

## CAG and Ubc, but not EF1α promoters, resist silencing in the TK4 vector

It has long been known that the choice of promoters greatly influences the degree of transgene silencing. We therefore tested three widely used promoters that are considered strong promoters in various contexts. CAG, ubiquitin C (Ubc), EF1α, and EF1α with additional specificity protein 1 (SP1) binding sites (herein referred to as long EF1α) were cloned into the TK4 vector in front of EGFP. We integrated these constructs into iPS cells and differentiated them into neurons with Ngn2. Flow cytometry analysis replicated that the CAG promoter resists silencing of EGFP (Figures 1F and S1C). Longitudinal confocal microscopy showed similar results (Figure S1D). In addition, the Ubc promoter was comparable to the CAG promoter. By contrast, both EF1α and long EF1α promoters were rapidly silenced. Notably, EGFP expression in undifferentiated stem cells was severalfold higher with the EF1α promoters than with CAG or Ubc, but this could not compensate for the high degree of silencing after neuronal differentiation (Figures S1H and S1I). Flow cytometry GFP histograms showed a uniform decrease in intensity across the whole population with both EF1α and long EF1α promoters at 3-week neurons (Figure 1H).

## The WPRE is a critical element to prevent silencing

To further assess the contribution of the vector elements to the prevention of silencing of the TK4 vector, we eliminated either the WPRE[24] or the poly(A) signal sequence from our PiggyBac vector. The construct without WPRE showed a strong decrease in GFP expression, whereas removing the poly(A) signal did not significantly affect the expression level during neuronal differentiation (Figures 1G, 1H, S1E, S1F, and S1J). This trend remained consistent for up to 8 weeks after differentiation (Figure S1K). qPCR analysis showed that mRNA expression also decreased during differentiation when the construct lacked WPRE (Figure S1L). In alignment with our previous results, mTagBFP2 expression driven by the EF1α promoter without WPRE decreased rapidly in all conditions (Figure S1G).

## Silencing in undifferentiated cells is also prevented by the TK4 vector

Since transgene silencing has been reported even in undifferentiated pluripotent stem cells within a few weeks,[25] we maintained iPS cells carrying the TK4 vector for 6 weeks without antibiotic selection to assess potential silencing of the EF1α-blue fluorescent protein (BFP) or the CAG-GFP-WPRE constructs in the undifferentiated state. In the absence of puromycin, a BFP-negative population gradually increased over the 6-week period. Unlike silencing during differentiation, which involves the entire population, here we found an ON-OFF silencing pattern: a cell population that silences the transgenes completely and another population that continues to express the same high levels (Figure 1I). As expected, the CAG-GFP transgene was not silenced during iPS cell expansion (Figure 1J). Of note, we observed a similar behavior of the TK4 vector without the WPRE, suggesting that WPRE is not necessary to prevent silencing of undifferentiated cells, unlike during differentiation (Figure 1J). Quantification of negative populations showed a significant increase in BFP-negative cells over 42 days of iPS cell maintenance without antibiotics, whereas the GFP-negative population remained unchanged between lines with or without antibiotics (Figure 1K). Since the silenced cell fraction was minor, the measurement of median flow cytometry intensity did not capture this ON-OFF silencing pattern (Figure S1M).

## No major contribution of insulator sequences to prevent silencing resistance

Since our TK4 vector contains several transcriptional insulators, we hypothesized that they may contribute to the prevention of transcriptional silencing. First, we removed all four insulators from our vector, creating a "Null" insulator version of our vector, and compared EGFP expression between the original TK4 vector and the Null vector (Figure 2A). Our flow cytometry and longitudinal imaging data showed that the insulators in the TK4 vector were not required to prevent silencing, unlike the WPRE (Figures 2B, S2A, and S2C). Unexpectedly, the TK4 vector without any insulator elements performed very similarly to the original TK4 vector.

Nevertheless, we wondered whether different variations of insulator additions may further improve the performance of the TK4 vector. We selected four insulator elements: the full-length 1.2 kb long chicken hypersensitive site 4 element

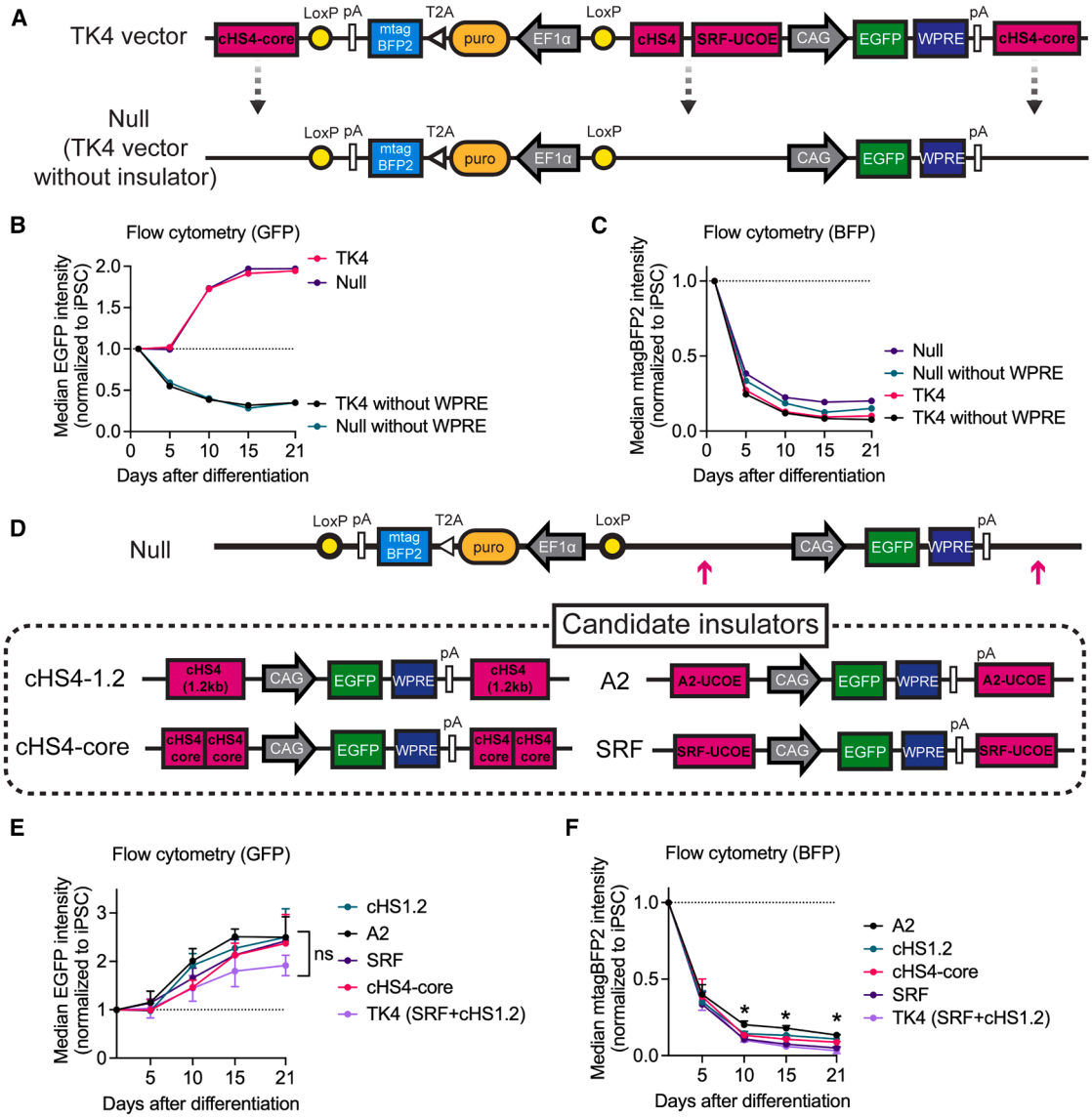


**Figure 2. No major impact of insulator sequences on maintaining gene expression from the TK4 vector during differentiation**

(A) The insulator sequences were eliminated from the TK4 vector to generate the TK4 Null vector.

(B) Median EGFP intensity measured by flow cytometry for each construct, with or without insulators and with or without WPRE, following neuronal differentiation; $n = 1$. Biological replicates are shown in Figure S2A.

(C) Median BFP intensity measurements corresponding to EGFP measurements shown in (B); $n = 1$. Biological replicates are shown in Figure S2B.

(D) Candidate insulators were inserted into the Null line at the position indicated.

(E) Median EGFP intensity showed no significant difference between constructs with different insulator elements during neuronal differentiation. Statistical analysis was performed using two-way ANOVA ($n = 3$). Data are shown as mean ± SD.

(F) Median BFP intensity was silenced in all vectors tested. Significant differences were observed between *A2 vs. SRF and *A2 vs. TK4 at day 10; *A2 vs. SRF, *A2 vs. TK4, *A2 vs. cHS4-core, ***SRF vs. cHS1.2, *TK4 vs. cHS4-core, *SRF vs. TK4, and ****TK4 vs. cHS1.2 at day 15; and **A2 vs. cHS4-core, **A2 vs. SRF, *A2 vs. TK4, and *SRF vs. cHS4-core at day 21. *$p < 0.05$, **$p < 0.01$, ***$p < 0.001$, ****$p < 0.0001$; two-way ANOVA with Tukey's multiple comparisons test; $n = 3$. Data are shown as mean ± SD.

See also Figure S2.

(referred to as cHS1.2),[15] the core of cHS4 (cHS4-core),[26] A2-UCOE,[5] and SRF-UCOE.[22] cHS4 acts as an insulator with specific protein binding sites to block heterochromatin spread, while UCOEs use housekeeping gene promoters to create ubiquitously active chromatin regions. We compared these insulators in different configurations, including flanking, upstream, and in the opposite orientation, using confocal microscopy (Figure S2D). However, no significant differences were observed between these configurations (Figures S2E and S2F). Next, we chose four constructs that tended to perform better than the original TK4 vector and tested them by flow cytometry. These constructs contained the four

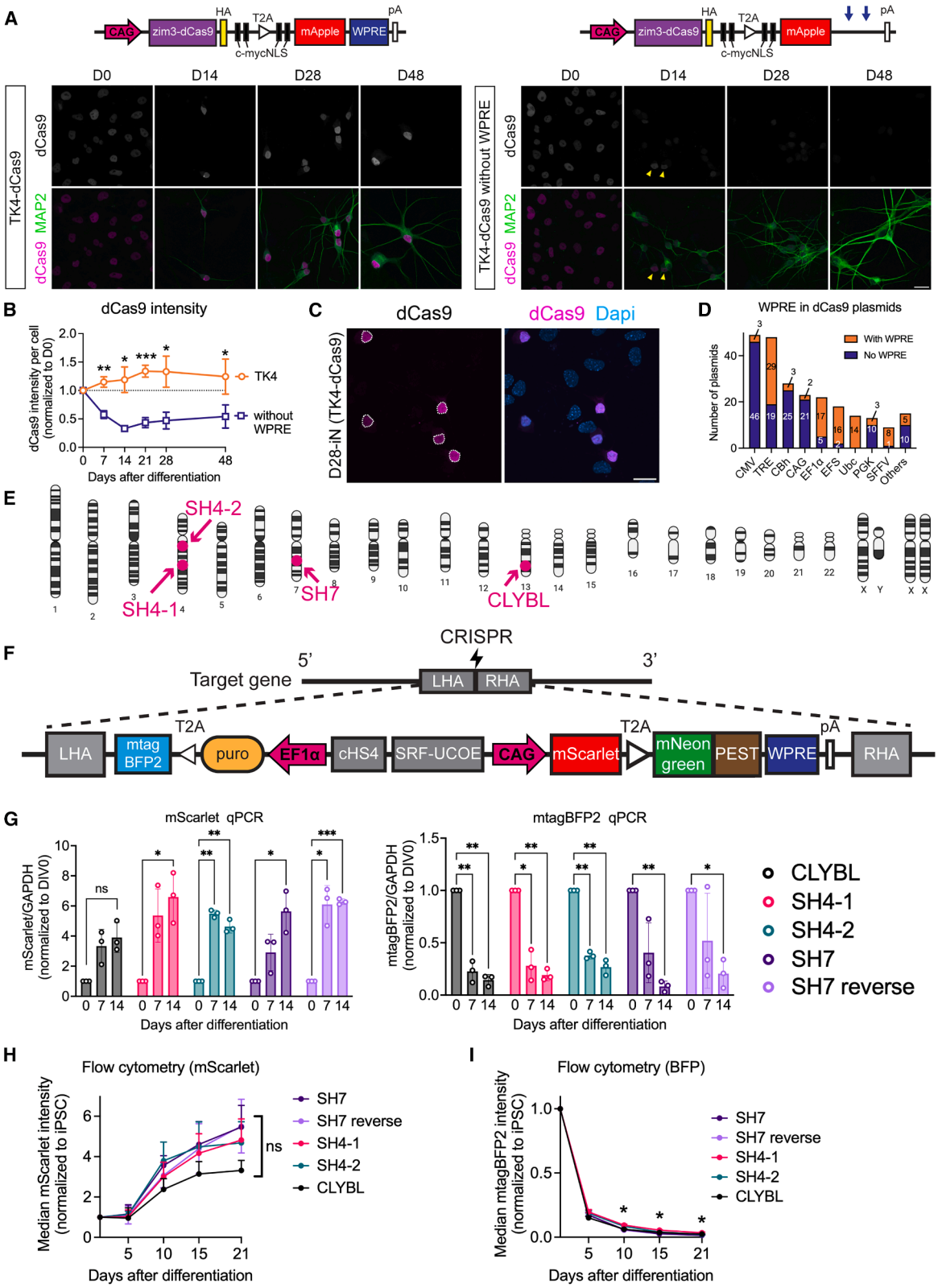


**Figure 3. TK4 enables stable transgene expression via both random and targeted integration into three new safe harbor loci**

(A) Zim3-dCas9 constructs with or without WPRE were integrated into iPS cells, followed by neuronal differentiation for 48 days. Representative immunostaining images with anti-dCas9 and microtubule-associated protein 2 (MAP2) antibodies are shown. Yellow arrows indicate residual dCas9 expression in cells with weak MAP2 signal at day 14 neurons in TK4 without WPRE. Scale bar, 20 μm.

*(legend continued on next page)*

insulators in a flanking position (Figure 2D). Again, there was a trend that these constructs lead to higher expression levels than the original TK4 vector upon differentiation, but the differences were not statistically significant (Figure 2E). As expected, mTagBFP2 intensity in these lines that contained these various insulators showed consistent silencing during differentiation as measured by flow cytometry since the insulators were positioned around GFP but not BFP (Figures 2C, 2F, and S2B). These data suggest that insulator elements may not be as critical as promoters or the WPRE for stable transgene expression during neuronal differentiation.

## The TK4 vector prevents silencing of non-EGFP transgenes, including dCas9

Next, we wanted to test another reporter gene in order to ensure that the effects observed so far are not unique to EGFP. We decided to first use the red fluorescent protein mScarlet, followed by a destabilized mNeonGreen protein joined with a T2A sequence that is predicted to produce two separate proteins. The inclusion of the destabilized mNeonGreen was an attempt to obtain a more sensitive expression readout than with stable fluorescent proteins. However, upon integration into iPS cells, we found that the destabilized mNeonGreen:proline, glutamic acid, serine, and threonine-rich (PEST) protein was so lowly expressed that it was impossible to distinguish it from the small amount of mScarlet bleed-through into the green channel and therefore focused only on measuring mScarlet for the quantification of transgene silencing. For best comparison with the EGFP results, we first cloned the mScarlet-mNeonGreen expression cassette into the identical TK4 PiggyBac vector (Figure S3A). Flow cytometry confirmed that mScarlet fluorescence increased rather than decreased during neuronal differentiation, even more than what we had previously observed for EGFP (Figure S3A).

Next, we wondered how a transgene coding for a non-fluorescent protein would perform in the TK4 vector. To this end, we cloned the commonly used CRISPR interference reagent dCas9-Zim3 tagged with hemagglutinin (HA) or mScarlet into the TK4 PiggyBac vector (Figure S3B). On days 14 and 40 of neuronal differentiation, we confirmed that almost all neurons exhibited mScarlet fluorescence (Figure S3B, top left and top middle). Furthermore, we also stained neurons at day 14 with anti-dCas9 and anti-HA antibodies to detect the HA-tagged dCas9 construct. Flow cytometry demonstrated that dCas9 and HA intensity were similar between differentiated neurons and undifferentiated iPS cells (Figure S3B, top right and bottom left). Thus, the TK4 vector also prevents silencing of non-fluorescent protein reporters.

Next, we wondered whether the WPRE is as important in the context of a dCas9 transgene as for EGFP. To this end, we transfected iPS cells with zinc finger imprinted 3 (Zim3)-dCas9 TK4 vectors with or without the WPRE and differentiated them to neurons and measured the amount of dCas9 by quantitative immunofluorescence up to 48 days. We found that dCas9 levels were stably maintained for 48 days of neuronal differentiation in the TK4 vector, whereas it got silenced in TK4 without WPRE (Figures 3A and 3B). A recent study found that some dCas9 constructs lead to non-nuclear localization during neuronal differentiation.[27] We confirmed that the double Myc nuclear localization signal in our construct led to efficient nuclear localization during the entire differentiation period (Figures 3A and 3C).

We have now observed that the combination of CAG and WPRE effectively prevents transgene silencing in several contexts. Given that both elements are well established and present in many expression constructs, we wondered how often CAG-WPRE vectors are used by the research community. We analyzed all 239 dCas9 expression plasmids deposited at Addgene that were requested at least 20 times (Table S1). CMV, tetracycline-responsive operator (TetO), CAG/hybrid cytomegalovirus enhancer/chicken β-actin (CBh) (a shorter version of CAG), and EF1α/elongation factor 1 alpha short (EFS) (a shorter version of EF1α) were the four main promoters used (Figure S3C). Strikingly, over 90% of CAG/CBh plasmids did not contain the WPRE (Figure 3D). Constructs with other promoters, such as CMV, used WPRE more often, resulting in nearly 60% of all 239 plasmids lacking the WPRE (Figure S3D). Thus, most constructs currently deposited at Addgene are not optimal for achieving stable dCas9 expression during differentiation.

## Three novel genomic loci for stable transgene expression

Next, we wanted to compare the performance of the expression cassette in the TK4 vector in various defined genomic loci in hopes of identifying a locus that may outperform popular

(B) dCas9 intensity per cell was normalized to iPS cells and measured over time in two cell lines. Significant differences were observed between TK4-dCas9 with vs. without WPRE. *$p < 0.05$, **$p < 0.01$, ***$p < 0.001$; two-way ANOVA with Tukey's multiple comparisons test; $n = 3$. Data are shown as mean ± SD.
(C) Representative immunostaining with anti-dCas9 antibody and DAPI showing nuclear localization of dCas9 in 4-week neurons. DAPI indicates mouse glia (large nuclei) and human neurons (small nuclei). Scale bar, 20 μm.
(D) Bar plots showing promoters used for dCas9 expression among 239 plasmids deposited at Addgene and requested more than 20 times. Purple indicates plasmids without WPRE, and orange indicates plasmids with WPRE. "Others" includes LTR ($n = 5$), MSCV ($n = 4$), SV40 ($n = 4$), and SYN ($n = 2$).
(E) The *CLYBL* and three novel safe harbor loci, distant from annotated genes, were selected for targeted integration of the TK4 expression cassette.[12]
(F) The expression construct of the TK4 vector was placed between targeting homology arms for CRISPR-mediated homologous recombination. Note: the destabilized mNeonGreen:PEST fluorescence was not detected by flow cytometry or microscopy and therefore not further evaluated.
(G) RT-qPCR analysis of mScarlet and mTagBFP2 at days 0 (iPS cells), 7, and 14 of neuronal differentiation. *$p < 0.05$, **$p < 0.01$, ***$p < 0.001$; two-way ANOVA with Dunnett's multiple comparisons test. $n = 3$. Data are shown as mean ± SD.
(H) Flow cytometry was used to measure the median mScarlet intensity during neuronal differentiation, normalized to the intensity in undifferentiated iPS cells for each targeted line. Statistical analysis was conducted using two-way ANOVA. $n = 3$. Data are shown as mean ± SD.
(I) Median BFP intensity in the indicated lines, equivalent to the analysis in (H). Significant differences were observed between *CLYBL vs. SH4-1, *SH4-1 vs. SH4-2, and SH4-1 vs. SH7 reverse at day 10; *CLYBL vs. SH4-1, *CLYBL vs. SH7, *CLYBL vs. SH7 reverse, *SH4-1 vs. SH4-2, **SH4-1 vs. SH7, **SH4-1 vs. SH7 reverse, **SH4-2 vs. SH7, and **SH4-2 vs. SH7 reverse at day 15; and **CLYBL vs. SH7, ***CLYBL vs. SH7 reverse, *SH4-1 vs. SH7, *SH4-2 vs. SH7, and *SH4-2 vs. SH7 reverse at day 21. *$p < 0.05$, **$p < 0.01$, ***$p < 0.001$; two-way ANOVA with Tukey's multiple comparisons test; $n = 3$. Data are shown as mean ± SD. See also Figure S3 and Table S1.

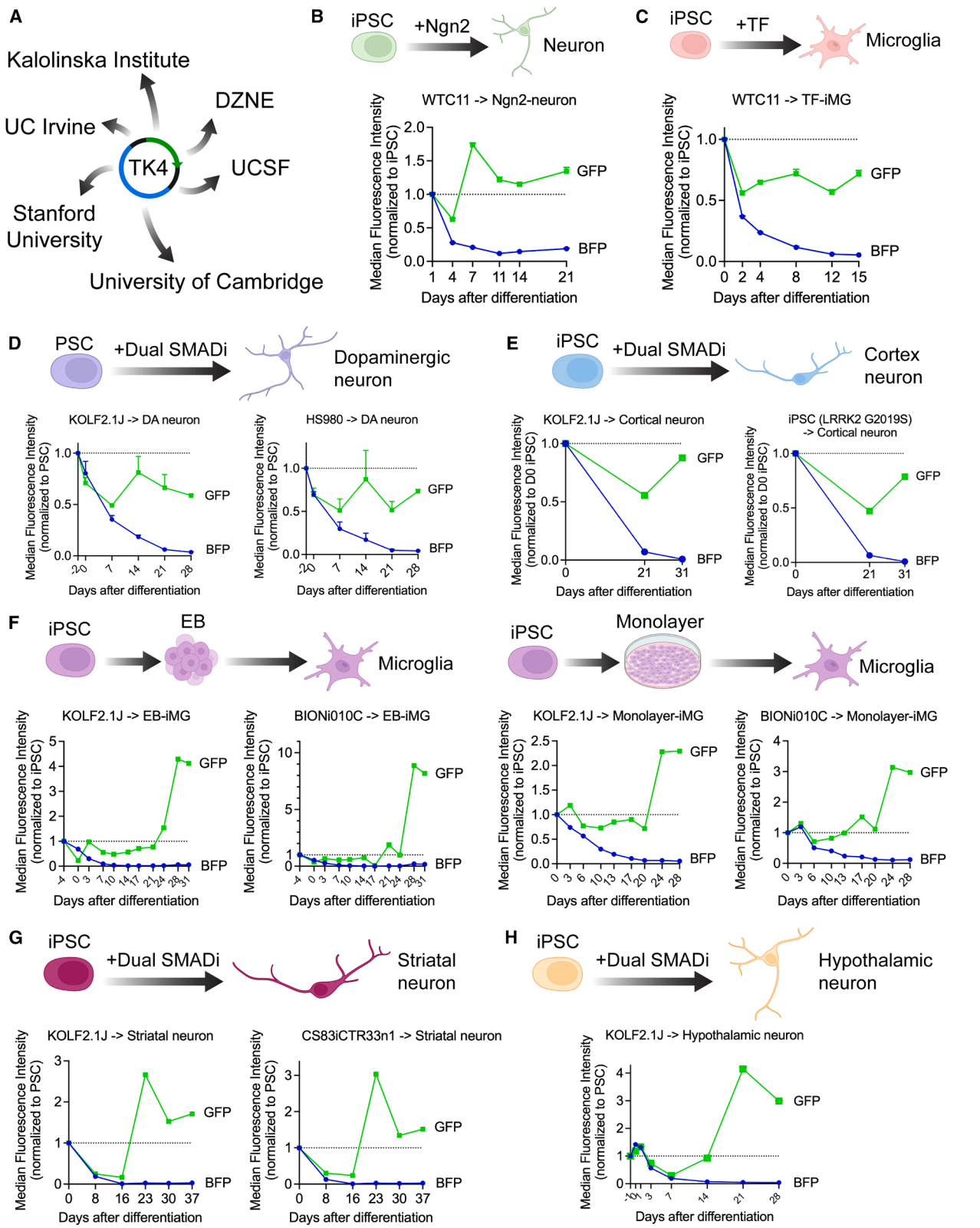


**Figure 4. The TK4 vector resists silencing among various neuronal and microglial differentiation protocols**

(A) The TK4 vector was distributed to six different laboratories. Each lab transfected the vector into various iPS cell lines and performed differentiation into neurons or microglia using different protocols. EGFP and BFP fluorescence was measured by flow cytometry and normalized to the expression level of undifferentiated iPS cells.

*(legend continued on next page)*

integration sites such as the CLYBL locus, which shows silencing of transgenes during neuronal differentiation (Figures 1B and 1C). Moreover, most current "safe" harbor sites do in fact destroy existing genes. A recent study developed a barcoded synthetic core promoter reporter integrated randomly by PiggyBac to measure the level of transcriptional support across thousands of sites in the human genome during the first 5 days of neuronal differentiation of iPS cells.[12] Among these characterized integration sites, we chose three that would represent good candidates of safe harbor locations. From the high-confidence integration sites reported, we chose three that were (1) in the "on-on group" (group 2 in that study) that were active in both iPS cells and in differentiated neurons, (2) in intergenic regions and distant from annotated genes, and (3) showed the highest expression levels (maximal cDNA/gDNA ratio). Two of these sites were on chromosome 4 and one on chromosome 7 (Figure 3E).

We identified CRISPR cut sites in the vicinity of these loci and generated targeting constructs by amplifying and cloning homology arms for these three loci into the TK4 vector (Figures 3F, S3E, and S3F). Transient nucleofection of guide-RNA/Cas9 ribonuclear protein (RNP) complexes facilitated the homologous recombination of expression constructs. For the chromosome 7 integration site, we generated the knock-ins in both orientations. After puromycin drug selection, iPS cell clones were picked and genotyped for proper transgene integration.

Next, we assessed mScarlet expression in five iPS cell lines with mScarlet targeted to the two sites on chromosome 4, the site on chromosome 7 in both orientations, and the CLYBL locus as a comparison. RT-qPCR analysis showed that mScarlet mRNA even increased following neuronal differentiation across all loci tested. In contrast and as expected, mTagBFP2 mRNA expression decreased progressively over time (Figure 3G). Consistent with the mRNA expression results, mScarlet fluorescence measured by flow cytometry showed an increase over time following neuronal differentiation (Figure 3H), while mTagBFP2 expression was rapidly silenced (Figure 3I). Compared with the CLYBL locus, our candidate loci showed a stronger and significant increase over time at the RNA level and a non-significant increase at the protein level. Especially, both orientations of the transgene integration at chromosome 7 resulted in non-significant but consistently higher mScarlet fluorescence among three biological replicates than the CLYBL integration site.

These data illustrate that our three novel safe harbor loci serve as excellent expression loci, at least on par with the CLYBL locus. In all loci, the expression elements of the TK4 vector prevented transgene silencing. With regard to overall expression levels, the three novel loci slightly outperformed the CLYBL locus, at least at the RNA level.

In addition, all three of our new loci are outside of any annotated transcriptional units, offering safer options for defined genomic integrations than currently used loci, especially in a therapeutic context.

### The TK4 vector resists silencing in various neuronal subtype cells and microglia derived from iPS cells, as assessed by seven different laboratories

Finally, we wanted to explore whether our results could be applied to additional cell types and differentiation protocols and are consistent between different laboratories. To address this, we shipped our TK4 PiggyBac vector to six additional labs in the US and Europe (Figure 4A). Researchers independently created TK4-integrated human iPS cells in 1 or 2 different cell lines and differentiated them into Ngn2-iN cells (Figure 4B), transcription factor-programmed microglia[28] (Figure 4C), dopaminergic neurons[29] (Figures 4D and S4B), cortical neurons[30,31] (Figures 4E and S4A), microglia using an embryoid body-based protocol[32] (Figure 4F), microglia using a monolayer-based protocol[33] (Figure 4F), striatal neurons[34] (Figures 4G and S4C), and hypothalamic neurons[35] (Figure 4H). Each group independently measured transgene expression over time during differentiation by flow cytometry as described above. Remarkably, without exception, the TK4 vector consistently showed stable or increased EGFP expression over time, while mTagBFP2 was silenced, in aggregate, in six different human iPS cell lines and nine different protocols. We conclude that the stable gene expression of the TK4 vector during neuronal and microglial differentiation of human iPS cells is robust and highly reproducible.

## DISCUSSION

We have established the TK4 PiggyBac system that effectively prevents transgene silencing during the differentiation of neurons or microglia from human stem cells. This construct has also proven useful for targeting specific loci, with reproducible results across various differentiation protocols conducted by different laboratories.

The silencing of experimental transgenes during differentiation of human pluripotent stem cells is a not much publicized but widely known problem in stem cell biology labs and, unfortunately, often rediscovered by scientists new to the field. Even simple genetic approaches, like expression of disease genes or genetic rescue of gene knockout experiments, often become unfeasible, let alone the use of sensors such as voltage or $Ca^{2+}$ indicators or Cas9-related enzymes for gene manipulation. Choosing strong constitutive promoters, targeting defined expression loci, or using

(B) Ngn2-neuronal mono-culture from the WTC11 iPS cell line; $n = 1$ with six technical replicates. Data are shown as mean ± SD.
(C) Transcription factor (TF)-mediated differentiation to microglia from the WTC11 line; $n = 1$ with three technical replicates. Data are shown as mean ± SD.
(D) Dopaminergic neurons from KOLF2.1J and HS980 stem cell lines; $n = 2$ for each line. Data are shown as mean ± SD.
(E) Cortical neurons from two different human iPS cell lines; $n = 1$ for each line.
(F) Microglia derived through an embryoid body (EB)-containing and a monolayer differentiation protocol from KOLF2.1J and BIONi010C iPS cell lines; $n = 1$ for each condition.
(G) Striatal neurons generated from KOLF2.1J and CS83iCTR33n1 iPS cell lines; $n = 1$ for each line.
(H) Hypothalamic neurons from KOLF2.1J line; $n = 1$ with three technical replicates. Data are shown as mean ± SD.
See also Figure S4.

insulator elements has resulted in highly stable transgene expression in pluripotent stem cells as long as they remain undifferentiated.[36–38] Remarkably, though, transgenic silencing will invariably occur during differentiation into somatic cell types.[4,39,40] At this point, the mechanisms of transgene silencing during pluripotent cell differentiation are not understood. Pluripotent cells are in a unique epigenetic state. E.g., they contain bivalent histone domains, and in contrast to somatic cells, they can tolerate complete loss of DNA methylation, loss of histone methylases like G9a, and loss of the RNAi machinery.[41–45] Of note, γ-retroviruses are acutely silenced in pluripotent and early embryonic cells, and the silencing is mediated by DNA methylation.[46,47] Perhaps when cells leave this unique epigenetic state as they exit pluripotency, decisive epigenetic changes need to be set in motion that overwhelm experimental expression cassettes, no matter where they are integrated.

Of note, transgene silencing has also been observed in undifferentiated pluripotent cells without the context of differentiation.[25,48–51] We found that silencing in undifferentiated cells occurs with EF1α, but not CAG promoters. Intriguingly, the silencing pattern observed in iPS cells showed a bi-modal ON-OFF pattern in contrast to differentiating cells, which showed a gradual silencing of the entire population. Accordingly, silencing in undifferentiated cells is best measured by the fraction of transgene-negative cells, whereas silencing in differentiating cells is better assessed by intensity with single-cell resolution.

Unlike previous studies, we did not observe a strong effect of insulators to prevent transgene silencing during differentiation.[5,52] This discrepancy may be due to technical differences. For example, one study[52] measured the percentage of GFP-positive cells rather than GFP intensity. In addition, the combination of the CAG promoter with the WPRE may have masked the contribution of insulators in preventing silencing. A more sensitive configuration, such as the EF1α promoter without WPRE, may allow for clearer differentiation in the effectiveness of various insulator elements.

Silencing has been mostly studied in highly proliferative cell lines. Like in pluripotent cells, epigenetic mechanisms, including DNA and histone methylation, have been implicated along with cell cycle-related mechanisms like R-loop formation, engagement of viral and transposon responses, and spreading of nearby heterochromatin.[39] Since cell proliferation rather decreases during neuronal differentiation, it is unlikely that cell cycle-related mechanisms are relevant. We observed no silencing of our randomly integrating PiggyBac vector in four different genomic loci. Moreover, various insulator sequences tested had little effect on transgene silencing. Hence, positional variegation effects such as heterochromatin spreading may also be of less importance in our system. Instead, we found that the combination of CAG or Ubc promoter sequences and the WPRE was primarily responsible for the prevention of downregulation of transgenes. In accordance with our findings, a recent paper used a CAG-WPRE construct to successfully express transgenes during cardiomyocyte differentiation of iPS cells.[53] The sequences of promoters are known to influence gene silencing. In particular, viral elements such as CMV, spleen focus-forming virus (SFFV), and γ-retroviral LTR promoters are subject to substantial silencing in mammalian cells.[54,55] However, even mammalian promoters that express well and stably in undifferentiated cells, such as EF1α or Ubc, silence upon differentiation without the WPRE. While the Eukaryotic translation elongation factor 1 alpha 1 (*EEF1A1*) gene is actively transcribed in mature neurons, it is known to be downregulated during differentiation of pluripotent stem cells.[56] Therefore, the strong and rapid decrease in transgene expression observed with the EF1α promoter is likely due to a combination of physiological downregulation and an active silencing mechanism of exogenous transcriptional DNA elements.[57] Remarkably, however, a subset of these stable promoters will resist silencing if the expression cassette is combined with a WPRE (Figures 1G, 3A, 3B, and S1J–S1L). The molecular mechanisms of how the WPRE increases cytoplasmatic mRNA are poorly understood. Based on sequence similarity to the Hepatitis B Virus PRE, it is assumed that it enhances nuclear export of mRNA.[58] Other potential mechanisms proposed include the support of transcriptional termination and 3′ RNA processing.[24,59] Thus, the effect of the WPRE in our context may rather represent an enhancement of transcription countering actively ongoing silencing mechanisms. Since all of these mechanisms are promoter independent, our observation that the WPRE only blocks silencing when combined with certain promoters suggests the existence of yet additional mechanisms for the WPRE's function. Perhaps it interacts with the 5′ end of the transcribed RNA molecule, such as transcriptional looping, which can result in transcriptional stabilization and depends on promoter sequences.[60]

Regarding polyadenylation, we found that removal of the poly(A) signal from TK4 had minimal effects on GFP expression. By contrast, efficient transcription termination and polyadenylation are generally required for robust gene expression.[61] One possible explanation is that an ill-defined cryptic poly(A) site is present in our vector. To ensure reliable transcription termination, we therefore retained the poly(A) sequence in the final version of the TK4 vector.

For both experimental and therapeutic applications, there is much debate about the characteristics of an optimal "safe harbor" site in the genome that can be used to express transgenes.[62] Due to unpredictable effects on transgenes targeted to gene deserts, the field has mostly used integrations into human genes considered less important (such as CLYBL, AAVS1, ROSA26, and C-C motif chemokine receptor 5 (CCR5) loci). These sites may be safe to ensure expression, but they are certainly not perfectly safe from a perspective of minimal interference with the host genome, as they all disrupt endogenous human genes. In this study, we took advantage of a recently developed resource that mapped genome-wide integration sites with the level of gene expression.[12] We purposely chose three novel candidate integrations that were distant from any annotated human genes and therefore have a greater potential to be actual safe harbor sites. All three of these novel expression loci performed as well as the CLYBL locus in terms of expression levels, if not even better. If gene disruption of the conventional safe harbor sites is of concern, these new sites could be an attractive alternative.

In summary, we here have developed a silencing-resistant expression construct that we hope will have a major impact on the field, as it will enable experiments that require robust transgene expression in somatic cells differentiated from pluripotent stem cells.

## Limitations of the study

The main limitation of this study is that we currently do not know whether the TK4 vector will prevent silencing in all somatic cells that can be generated from human pluripotent stem cells. In this study, we only assessed neuronal and myeloid differentiation. We hope our vector will be tested by more scientists in the stem cell field to address this important question.

Another critical limitation of this study is the number of reporter genes tested. Most of our results are based on EGFP expression. In addition, we have confirmed that the red fluorescent protein mScarlet and dCas9 behave like EGFP. However, it has been seen before that the transgene used affects the degree of silencing. It is therefore likely that the TK4 will not be able to resist silencing of all transgenes.

Finally, the strong promoter dependence we observed will require us to test any additional promoters that may be desired, such as cell-type-specific or inducible promoters.

## RESOURCE AVAILABILITY

### Lead contact

Requests for reagents and resources reported in this article should be directed to and will be fulfilled by the lead contact, Marius Wernig (wernig@stanford.edu).

### Materials availability

The TK4 PiggyBac vector and the plasmids containing the homology arms to target the three novel safe harbor sites have been deposited to Addgene (TK4-NLS-EGFP, #239046; TK4-EGFP, #239047; and TBD). All other materials are available from the lead contact upon request.

### Data and code availability

- All data reported in this paper will be shared by the lead contact upon request.
- ImageJ scripts used to quantify EGFP or dCas9 fluorescence intensity are available from the lead contact upon request.
- Any additional information required to reanalyze the data reported in this paper is available from the lead contact upon request.

## ACKNOWLEDGMENTS

This work was conceptualized by the Chan-Zuckerberg-Initiative Neurodegeneration Challenge Network's Stem Cell Working Group, led by Margaret Sutherland, and supported by a grant from the Chan-Zuckerberg-Initiative. We would like to thank the FACS Core at the Institute for Stem Cell Biology and Regenerative Medicine of Stanford University and the Wu Tsai Neuroscience Institute Neuroscience Microscopy Service of Stanford University for their microscopy assistance, expertise, and services; Gang Ning for help with genotyping of clonal knockin cells and FACS; Lacramioara Bintu and Michael Bassik for critical comments on the manuscript; and Alaka Mullick, together with all members of the working group, for helpful discussions and comments on the study design and execution of this project. Hsiao-Jou Cortina Chen, Eugene Seah, and Amber Keith provided technical support. T.U. was supported by a postdoctoral scholar award from the Phil & Penny Knight Initiative for Brain Resilience at the Wu Tsai Neurosciences Institute, Stanford University, and by the Huntington's Disease Foundation. A.M. was supported by postdoctoral fellowships from the Alzheimer's Association (AARF-22-973222) and the Larry L. Hillblom Foundation (2022-A-016-FEL). A.J.S. was supported by the NIH/NIA Pathway to Independence Award (K99AG080116). L.E. was supported by the Studienstiftung des Deutschen Volkes (German Academic Scholarship Foundation, PhD Scholarship) and the International Max-Planck Research School for the Mechanisms of The Mental Function and Dysfunction (IMPRS-MMFD, PhD Scholarship). M.K. was independently supported by the Chan Zuckerberg Initiative (2022-316571). L.M.T. was supported by NIH grants (R35NS116872). A.R.B. was supported partially by Wellcome Core funding to the Sanger Institute (grant number 220540/Z/20/A). F.T.M. is a New York Stem Cell Foundation—Robertson Investigator (NYSCF-R-156) and was supported by a Chan Zuckerberg Initiative—Ben Barres Early Career Investigator award (CZI NDCN 191942, 10.37921/429861umrcjh) and a fellowship from the Wellcome Trust and Royal Society (211221/Z/18/Z). Funding for this work was provided, in part, through the National Institute of Neurological Disorders and Stroke (NINDS), NIH, and from the Chan Zuckerberg Initiative (M.E.W.).

## AUTHOR CONTRIBUTIONS

Conceptualization, M.W. and M.E.W.; methodology, M.W., M.E.W., and T.U.; investigation and formal analysis, T.U., A.N., A.D.S., D.S., A.S., E.C., J.C., L.E., A.M., D.R., A.R., L.S., A.J.S., K.S., N.J.W., K.W., and Q.W.; resources, W.C.S.; visualization, T.U., L.S., K.S., and N.J.W.; funding acquisition, M.W., M.E.W., W.C.S., L.M.T., B.S., F.T.M., D.K.-V., M.K., A.R.B., and E.A.; writing – original draft, M.W. and T.U.; writing – review and editing, M.W., T.U., J.C., L.E., A.M., L.S., A.J.S., K.S., N.J.W., E.A., A.R.B., M.K., D.K.-V., F.T.M., B.S., L.M.T., W.C.S., and M.E.W.

## DECLARATION OF INTERESTS

M.W. is a co-founder of Neucyte Inc., a scientific advisor for bit.bio Ltd., and co-founder and scientific advisor of Lytherian Therapeutics and Theseus Therapies. A.R.B. is a founder and consultant for Ensocell Therapeutics. M.K. is a co-scientific founder of Montara Therapeutics and serves on the Scientific Advisory Boards of Engine Biosciences, Alector, and Montara Therapeutics and is an advisor to Modulo Bio and Theseus Therapies.

## STAR★METHODS

Detailed methods are provided in the online version of this paper and include the following:

- KEY RESOURCES TABLE
- EXPERIMENTAL MODEL AND STUDY PARTICIPANT DETAILS
  - Cell lines
  - iPS Cell Culture and Generation of Polyclonal Lines Using PiggyBac Vector (Wernig lab)
  - iPS cell culture and nucleofections for gene targeting (Skarnes lab)
  - Human stem cells (Kampmann lab)
  - Stem cell culture (Arenas lab)
  - iPSC Culture (Kronenberg-Versteeg lab)
  - Stem Cell Culture (Thompson lab)
- METHOD DETAILS
  - Lentiviral generation
  - Generation of Ngn2-iN cells (Wernig lab)
  - Flow cytometry analysis (all participating labs)
  - Confocal microscopy analysis (Wernig lab)
  - Immunostaining and measurement of dCas9 intensity (Wernig lab)
  - RNA extraction and qRT-PCR (*Wernig lab*)
  - Genotyping (Skarnes lab)
  - Ngn2-neuron Differentiation (Kampmann lab)
  - 6TF-Microglia Differentiation (Kampmann lab)
  - Midbrain Dopaminergic Neuron Differentiation (Arenas lab)
  - Embryoid body-based Microglia Differentiation (Kronenberg-Versteeg lab)
  - Monolayer-based Microglia Differentiation (Kronenberg-Versteeg lab)
  - Final Microglia Differentiation and Maturation (Kronenberg-Versteeg lab)
  - Striatal Neuron Differentiation (Thompson lab)
  - Hypothalamic neuron differentiation (Merkle lab)
  - Cortical neuron differentiation (Schüle lab)
  - Flow cytometry analysis (Ward lab)
- QUANTIFICATION AND STATISTICAL ANALYSIS

## SUPPLEMENTAL INFORMATION

Supplemental information can be found online at https://doi.org/10.1016/j.stem.2026.01.007.

Received: September 17, 2024
Revised: October 30, 2025
Accepted: January 16, 2026
Published: February 13, 2026

## REFERENCES

1. Singh, V.K., Kalsan, M., Kumar, N., Saini, A., and Chandra, R. (2015). Induced pluripotent stem cells: applications in regenerative medicine, disease modeling, and drug discovery. Front. Cell Dev. Biol. *3*, 2. https://doi.org/10.3389/fcell.2015.00002.
2. Pfaff, N., Lachmann, N., Ackermann, M., Kohlscheen, S., Brendel, C., Maetzig, T., Niemann, H., Antoniou, M.N., Grez, M., Schambach, A., et al. (2013). A ubiquitous chromatin opening element prevents transgene silencing in pluripotent stem cells and their differentiated progeny. Stem Cells *31*, 488–499. https://doi.org/10.1002/stem.1316.
3. Ackermann, M., Lachmann, N., Hartung, S., Eggenschwiler, R., Pfaff, N., Happle, C., Mucci, A., Göhring, G., Niemann, H., Hansen, G., et al. (2014). Promoter and lineage independent anti-silencing activity of the A2 ubiquitous chromatin opening element for optimized human pluripotent stem cell-based gene therapy. Biomaterials *35*, 1531–1542. https://doi.org/10.1016/j.biomaterials.2013.11.024.
4. Karbassi, E., Padgett, R., Bertero, A., Reinecke, H., Klaiman, J.M., Yang, X., Hauschka, S.D., and Murry, C.E. (2024). Targeted CRISPR activation is functional in engineered human pluripotent stem cells but undergoes silencing after differentiation into cardiomyocytes and endothelium. Cell. Mol. Life Sci. *81*, 95. https://doi.org/10.1007/s00018-023-05101-2.
5. Müller-Kuller, U., Ackermann, M., Kolodziej, S., Brendel, C., Fritsch, J., Lachmann, N., Kunkel, H., Lausen, J., Schambach, A., Moritz, T., et al. (2015). A minimal ubiquitous chromatin opening element (UCOE) effectively prevents silencing of juxtaposed heterologous promoters by epigenetic remodeling in multipotent and pluripotent stem cells. Nucleic Acids Res. *43*, 1577–1592. https://doi.org/10.1093/nar/gkv019.
6. Hong, S., Hwang, D.-Y., Yoon, S., Isacson, O., Ramezani, A., Hawley, R.G., and Kim, K.-S. (2007). Functional Analysis of Various Promoters in Lentiviral Vectors at Different Stages of In Vitro Differentiation of Mouse Embryonic Stem Cells. Mol. Ther. *15*, 1630–1639. https://doi.org/10.1038/sj.mt.6300251.
7. Pannell, D., and Ellis, J. (2001). Silencing of gene expression: implications for design of retrovirus vectors. Rev. Med. Virol. *11*, 205–217. https://doi.org/10.1002/rmv.316.
8. Brooks, A.R., Harkins, R.N., Wang, P., Qian, H.S., Liu, P., and Rubanyi, G.M. (2004). Transcriptional silencing is associated with extensive methylation of the CMV promoter following adenoviral gene delivery to muscle. J. Gene Med. *6*, 395–404. https://doi.org/10.1002/jgm.516.
9. Seczynska, M., Bloor, S., Cuesta, S.M., and Lehner, P.J. (2022). Genome surveillance by HUSH-mediated silencing of intronless mobile elements. Nature *601*, 440–445. https://doi.org/10.1038/s41586-021-04228-1.
10. Garrison, B.S., Yant, S.R., Mikkelsen, J.G., and Kay, M.A. (2007). Postintegrative Gene Silencing within the *Sleeping Beauty* Transposition System. Mol. Cell. Biol. *27*, 8824–8833. https://doi.org/10.1128/MCB.00498-07.
11. Alhaji, S.Y., Ngai, S.C., and Abdullah, S. (2019). Silencing of transgene expression in mammalian cells by DNA methylation and histone modifications in gene therapy perspective. Biotechnol. Genet. Eng. Rev. *35*, 1–25. https://doi.org/10.1080/02648725.2018.1551594.
12. Wu, Q., Wu, J., Karim, K., Chen, X., Wang, T., Iwama, S., Carobbio, S., Keen, P., Vidal-Puig, A., Kotter, M.R., et al. (2023). Massively parallel characterization of CRISPR activator efficacy in human induced pluripotent stem cells and neurons. Mol. Cell *83*, 1125–1139.e8. https://doi.org/10.1016/j.molcel.2023.02.011.
13. Lombardo, A., Cesana, D., Genovese, P., Di Stefano, B., Provasi, E., Colombo, D.F., Neri, M., Magnani, Z., Cantore, A., Lo Riso, P., et al. (2011). Site-specific integration and tailoring of cassette design for sustainable gene transfer. Nat. Methods *8*, 861–869. https://doi.org/10.1038/nmeth.1674.
14. Hammond, S.M., Caudy, A.A., and Hannon, G.J. (2001). Post-transcriptional gene silencing by double-stranded RNA. Nat. Rev. Genet. *2*, 110–119. https://doi.org/10.1038/35052556.
15. Emery, D.W., Yannaki, E., Tubb, J., and Stamatoyannopoulos, G. (2000). A chromatin insulator protects retrovirus vectors from chromosomal position effects. Proc. Natl. Acad. Sci. USA *97*, 9150–9155. https://doi.org/10.1073/pnas.160159597.
16. Kotin, R.M., Linden, R.M., and Berns, K.I. (1992). Characterization of a preferred site on human chromosome 19q for integration of adeno-associated virus DNA by non-homologous recombination. EMBO J. *11*, 5071–5078. https://doi.org/10.1002/j.1460-2075.1992.tb05614.x.
17. Cerbini, T., Funahashi, R., Luo, Y., Liu, C., Park, K., Rao, M., Malik, N., and Zou, J. (2015). Transcription Activator-Like Effector Nuclease (TALEN)-Mediated CLYBL Targeting Enables Enhanced Transgene Expression and One-Step Generation of Dual Reporter Human Induced Pluripotent Stem Cell (iPSC) and Neural Stem Cell (NSC) Lines. PLoS One *10*, e0116032. https://doi.org/10.1371/journal.pone.0116032.
18. Jones, P.A., and Takai, D. (2001). The Role of DNA Methylation in Mammalian Epigenetics. Science *293*, 1068–1070. https://doi.org/10.1126/science.1063852.
19. Klein, H.-U., McCabe, C., Gjoneska, E., Sullivan, S.E., Kaskow, B.J., Tang, A., Smith, R.V., Xu, J., Pfenning, A.R., Bernstein, B.E., et al. (2019). Epigenome-wide study uncovers large-scale changes in histone acetylation driven by tau pathology in aging and Alzheimer's human brains. Nat. Neurosci. *22*, 37–46. https://doi.org/10.1038/s41593-018-0291-1.
20. Sun, Z., and Südhof, T.C. (2021). A simple Ca2+-imaging approach to neural network analyses in cultured neurons. J. Neurosci. Methods *349*, 109041. https://doi.org/10.1016/j.jneumeth.2020.109041.
21. Tian, R., Gachechiladze, M.A., Ludwig, C.H., Laurie, M.T., Hong, J.Y., Nathaniel, D., Prabhu, A.V., Fernandopulle, M.S., Patel, R., Abshari, M., et al. (2019). CRISPR Interference-Based Platform for Multimodal Genetic Screens in Human iPSC-Derived Neurons. Neuron *104*, 239–255.e12. https://doi.org/10.1016/j.neuron.2019.07.014.
22. Rudina, S.S., and Smolke, C.D. (2019). A Novel Chromatin-Opening Element for Stable Long-term Transgene Expression. Preprint at bioRxiv, 626713. https://doi.org/10.1101/626713.
23. Wang, C., Ward, M.E., Chen, R., Liu, K., Tracy, T.E., Chen, X., Xie, M., Sohn, P.D., Ludwig, C., Meyer-Franke, A., et al. (2017). Scalable Production of iPSC-Derived Human Neurons to Identify Tau-Lowering Compounds by High-Content Screening. Stem Cell Rep. *9*, 1221–1233. https://doi.org/10.1016/j.stemcr.2017.08.019.
24. Zufferey, R., Donello, J.E., Trono, D., and Hope, T.J. (1999). Woodchuck Hepatitis Virus Posttranscriptional Regulatory Element Enhances Expression of Transgenes Delivered by Retroviral Vectors. J. Virol. *73*, 2886–2892. https://doi.org/10.1128/JVI.73.4.2886-2892.1999.
25. Fitzgerald, M., Livingston, M., Gibbs, C., and Deans, T.L. (2020). Rosa26 docking sites for investigating genetic circuit silencing in stem cells. Synth. Biol. (Oxf.) *5*, ysaa014. https://doi.org/10.1093/synbio/ysaa014.
26. Chung, J.H., Bell, A.C., and Felsenfeld, G. (1997). Characterization of the chicken beta-globin insulator. Proc. Natl. Acad. Sci. USA *94*, 575–580. https://doi.org/10.1073/pnas.94.2.575.
27. Cajka, G., Liu, M., and Shalem, O. (2024). CRISPR associated enzymes are mislocalized to the cytoplasm in iPSC-derived neurons resulting in KRAB-specific degradation. Preprint at bioRxiv. 2024.10.19.619045. https://doi.org/10.1101/2024.10.19.619045.
28. Dräger, N.M., Sattler, S.M., Huang, C.T.-L., Teter, O.M., Leng, K., Hashemi, S.H., Hong, J., Aviles, G., Clelland, C.D., Zhan, L., et al. (2022). A CRISPRi/a platform in human iPSC-derived microglia uncovers regulators of disease states. Nat. Neurosci. *25*, 1149–1162. https://doi.org/10.1038/s41593-022-01131-4.

29. Pantazis, C.B., Yang, A., Lara, E., McDonough, J.A., Blauwendraat, C., Peng, L., Oguro, H., Kanaujiya, J., Zou, J., Sebesta, D., et al. (2022). A reference human induced pluripotent stem cell line for large-scale collaborative studies. Cell Stem Cell *29*, 1685–1702.e22. https://doi.org/10.1016/j.stem.2022.11.004.

30. Shi, Y., Kirwan, P., and Livesey, F.J. (2012). Directed differentiation of human pluripotent stem cells to cerebral cortex neurons and neural networks. Nat. Protoc. *7*, 1836–1846. https://doi.org/10.1038/nprot.2012.116.

31. Calatayud, C., Muñoz-Pedrazo, E., Fernández-Gallego, S., and Verstreken, P. (2022). Modular generation of cortical, striatal and ventral midbrain progenitor cells. Protocols.io. https://doi.org/10.17504/protocols.io.b54cq8sw.

32. Haenseler, W., Sansom, S.N., Buchrieser, J., Newey, S.E., Moore, C.S., Nicholls, F.J., Chintawar, S., Schnell, C., Antel, J.P., Allen, N.D., et al. (2017). A Highly Efficient Human Pluripotent Stem Cell Microglia Model Displays a Neuronal-Co-culture-Specific Expression Profile and Inflammatory Response. Stem Cell Rep. *8*, 1727–1742. https://doi.org/10.1016/j.stemcr.2017.05.017.

33. Takata, K., Kozaki, T., Lee, C.Z.W., Thion, M.S., Otsuka, M., Lim, S., Utami, K.H., Fidan, K., Park, D.S., Malleret, B., et al. (2017). Induced-Pluripotent-Stem-Cell-Derived Primitive Macrophages Provide a Platform for Modeling Tissue-Resident Macrophage Differentiation and Function. Immunity *47*, 183–198.e6. https://doi.org/10.1016/j.immuni.2017.06.017.

34. Smith-Geater, C., Hernandez, S.J., Lim, R.G., Adam, M., Wu, J., Stocksdale, J.T., Wassie, B.T., Gold, M.P., Wang, K.Q., Miramontes, R., et al. (2020). Aberrant Development Corrected in Adult-Onset Huntington's Disease iPSC-Derived Neuronal Cultures via WNT Signaling Modulation. Stem Cell Rep. *14*, 406–419. https://doi.org/10.1016/j.stemcr.2020.01.015.

35. Chen, H.C., Mazzaferro, S., Tian, T., Mali, I., and Merkle, F.T. (2023). Differentiation, Transcriptomic Profiling, and Calcium Imaging of Human Hypothalamic Neurons. Curr. Protoc. *3*, e786. https://doi.org/10.1002/cpz1.786.

36. Norrman, K., Fischer, Y., Bonnamy, B., Wolfhagen Sand, F.W., Ravassard, P., and Semb, H. (2010). Quantitative Comparison of Constitutive Promoters in Human ES cells. PLOS One *5*, e12413. https://doi.org/10.1371/journal.pone.0012413.

37. Benabdellah, K., Gutierrez-Guerrero, A., Cobo, M., Muñoz, P., and Martín, F. (2014). A chimeric HS4-SAR insulator (IS2) that prevents silencing and enhances expression of lentiviral vectors in pluripotent stem cells. PLoS One *9*, e84268. https://doi.org/10.1371/journal.pone.0084268.

38. Tay, F.C., Tan, W.K., Goh, S.-L., Ramachandra, C.J.A., Lau, C.-H., Zhu, H., Chen, C., Du, S., Phang, R.Z., Shahbazi, M., et al. (2013). Targeted transgene insertion into the AAVS1 locus driven by baculoviral vector-mediated zinc finger nuclease expression in human-induced pluripotent stem cells. J. Gene Med. *15*, 384–395. https://doi.org/10.1002/jgm.2745.

39. Cabrera, A., Edelstein, H.I., Glykofrydis, F., Love, K.S., Palacios, S., Tycko, J., Zhang, M., Lensch, S., Shields, C.E., Livingston, M., et al. (2022). The sound of silence: Transgene silencing in mammalian cell engineering. Cell Syst. *13*, 950–973. https://doi.org/10.1016/j.cels.2022.11.005.

40. Wolf, D., and Goff, S.P. (2009). Embryonic stem cells use ZFP809 to silence retroviral DNAs. Nature *458*, 1201–1204. https://doi.org/10.1038/nature07844.

41. Bernstein, B.E., Mikkelsen, T.S., Xie, X., Kamal, M., Huebert, D.J., Cuff, J., Fry, B., Meissner, A., Wernig, M., Plath, K., et al. (2006). A bivalent chromatin structure marks key developmental genes in embryonic stem cells. Cell *125*, 315–326. https://doi.org/10.1016/j.cell.2006.02.041.

42. Smith, A.G. (2001). Embryo-derived stem cells: of mice and men. Annu. Rev. Cell Dev. Biol. *17*, 435–462. https://doi.org/10.1146/annurev.cellbio.17.1.435.

43. Reik, W. (2007). Stability and flexibility of epigenetic gene regulation in mammalian development. Nature *447*, 425–432. https://doi.org/10.1038/nature05918.

44. Kanellopoulou, C., Muljo, S.A., Kung, A.L., Ganesan, S., Drapkin, R., Jenuwein, T., Livingston, D.M., and Rajewsky, K. (2005). Dicer-deficient mouse embryonic stem cells are defective in differentiation and centromeric silencing. Genes Dev. *19*, 489–501. https://doi.org/10.1101/gad.1248505.

45. Tachibana, M., Sugimoto, K., Nozaki, M., Ueda, J., Ohta, T., Ohki, M., Fukuda, M., Takeda, N., Niida, H., Kato, H., et al. (2002). G9a histone methyltransferase plays a dominant role in euchromatic histone H3 lysine 9 methylation and is essential for early embryogenesis. Genes Dev. *16*, 1779–1791. https://doi.org/10.1101/gad.989402.

46. Jähner, D., Stuhlmann, H., Stewart, C.L., Harbers, K., Löhler, J., Simon, I., and Jaenisch, R. (1982). De novo methylation and expression of retroviral genomes during mouse embryogenesis. Nature *298*, 623–628. https://doi.org/10.1038/298623a0.

47. Stewart, C.L., Vanek, M., and Wagner, E.F. (1985). Expression of foreign genes from retroviral vectors in mouse teratocarcinoma chimaeras. EMBO J. *4*, 3701–3709. https://doi.org/10.1002/j.1460-2075.1985.tb04138.x.

48. DiAndreth, B., Wauford, N., Hu, E., Palacios, S., and Weiss, R. (2022). PERSIST platform provides programmable RNA regulation using CRISPR endoRNases. Nat. Commun. *13*, 2582. https://doi.org/10.1038/s41467-022-30172-3.

49. Gödecke, N., Herrmann, S., Weichelt, V., and Wirth, D. (2023). A Ubiquitous Chromatin Opening Element and DNA Demethylation Facilitate Doxycycline-Controlled Expression during Differentiation and in Transgenic Mice. ACS Synth. Biol. *12*, 482–491. https://doi.org/10.1021/acssynbio.2c00450.

50. Gödecke, N., Zha, L., Spencer, S., Behme, S., Riemer, P., Rehli, M., Hauser, H., and Wirth, D. (2017). Controlled re-activation of epigenetically silenced Tet promoter-driven transgene expression by targeted demethylation. Nucleic Acids Res. *45*, e147. https://doi.org/10.1093/nar/gkx601.

51. Galat, V., Galat, Y., Perepitchka, M., Jennings, L.J., Iannaccone, P.M., and Hendrix, M.J.C. (2016). Transgene Reactivation in Induced Pluripotent Stem Cell Derivatives and Reversion to Pluripotency of Induced Pluripotent Stem Cell-Derived Mesenchymal Stem Cells. Stem Cells Dev. *25*, 1060–1072. https://doi.org/10.1089/scd.2015.0366.

52. Macarthur, C.C., Xue, H., Van Hoof, D., Lieu, P.T., Dudas, M., Fontes, A., Swistowski, A., Touboul, T., Seerke, R., Laurent, L.C., et al. (2012). Chromatin insulator elements block transgene silencing in engineered human embryonic stem cell lines at a defined chromosome 13 locus. Stem Cells Dev. *21*, 191–205. https://doi.org/10.1089/scd.2011.0163.

53. Wexler, Y., Grinstein, H., Huber, I., Glatstein, S., Ghiringhelli, M., Edri, O., Landesberg, M., Shiff, D., Arbel, G., Rosh, I., et al. (2025). XPRESSO: Rapid genetic engineering of human pluripotent stem cells for durable overexpression using a modular anti-silencing vector. Stem Cell Rep. *20*, 102603. https://doi.org/10.1016/j.stemcr.2025.102603.

54. Herbst, F., Ball, C.R., Tuorto, F., Nowrouzi, A., Wang, W., Zavidij, O., Dieter, S.M., Fessler, S., van der Hoeven, F., Kloz, U., et al. (2012). Extensive methylation of promoter sequences silences lentiviral transgene expression during stem cell differentiation in vivo. Mol. Ther. *20*, 1014–1021. https://doi.org/10.1038/mt.2012.46.

55. Teschendorf, C., Warrington, K.H., Siemann, D.W., and Muzyczka, N. (2002). Comparison of the EF-1 alpha and the CMV promoter for engineering stable tumor cell lines using recombinant adeno-associated virus. Anticancer Res. *22*, 3325–3330.

56. DePuy, S.D., Stornetta, R.L., Bochorishvili, G., Deisseroth, K., Witten, I., Coates, M., and Guyenet, P.G. (2013). Glutamatergic neurotransmission between the C1 neurons and the parasympathetic preganglionic neurons of the dorsal motor nucleus of the vagus. J. Neurosci. *33*, 1486–1497. https://doi.org/10.1523/JNEUROSCI.4269-12.2013.

57. Battulin, N., Korablev, A., Ryzhkova, A., Smirnov, A., Kabirova, E., Khabarova, A., Lagunov, T., Serova, I., and Serov, O. (2022). The human EF1a promoter does not provide expression of the transgene in mice. Transgen. Res. *31*, 525–535. https://doi.org/10.1007/s11248-022-00319-5.

58. Donello, J.E., Loeb, J.E., and Hope, T.J. (1998). Woodchuck hepatitis virus contains a tripartite posttranscriptional regulatory element. J. Virol. *72*, 5085–5092. https://doi.org/10.1128/JVI.72.6.5085-5092.1998.

59. Higashimoto, T., Urbinati, F., Perumbeti, A., Jiang, G., Zarzuela, A., Chang, L.J., Kohn, D.B., and Malik, P. (2007). The woodchuck hepatitis virus post-transcriptional regulatory element reduces readthrough transcription from retroviral vectors. Gene Ther. *14*, 1298–1304. https://doi.org/10.1038/sj.gt.3302979.

60. Grzechnik, P., Tan-Wong, S.M., and Proudfoot, N.J. (2014). Terminate and make a loop: regulation of transcriptional directionality. Trends Biochem. Sci. *39*, 319–327. https://doi.org/10.1016/j.tibs.2014.05.001.

61. Colgan, D.F., and Manley, J.L. (1997). Mechanism and regulation of mRNA polyadenylation. Genes Dev. *11*, 2755–2766. https://doi.org/10.1101/gad.11.21.2755.

62. Papapetrou, E.P., and Schambach, A. (2016). Gene Insertion Into Genomic Safe Harbors for Human Gene Therapy. Mol. Ther. *24*, 678–684. https://doi.org/10.1038/mt.2016.38.

63. Zhang, Y., Pak, C., Han, Y., Ahlenius, H., Zhang, Z., Chanda, S., Marro, S., Patzke, C., Acuna, C., Covy, J., et al. (2013). Rapid single-step induction of functional neurons from human pluripotent stem cells. Neuron *78*, 785–798. https://doi.org/10.1016/j.neuron.2013.05.029.

64. Hockemeyer, D., Soldner, F., Cook, E.G., Gao, Q., Mitalipova, M., and Jaenisch, R. (2008). A drug-inducible system for direct reprogramming of human somatic cells to pluripotency. Cell Stem Cell *3*, 346–353. https://doi.org/10.1016/j.stem.2008.08.014.

65. Dull, T., Zufferey, R., Kelly, M., Mandel, R.J., Nguyen, M., Trono, D., and Naldini, L. (1998). A third-generation lentivirus vector with a conditional packaging system. J. Virol. *72*, 8463–8471. https://doi.org/10.1128/JVI.72.11.8463-8471.1998.

66. Skarnes, W.C., Pellegrino, E., and McDonough, J.A. (2019). Improving homology-directed repair efficiency in human stem cells. Methods *164*, 18–28. https://doi.org/10.1016/j.ymeth.2019.06.016.

67. Miyaoka, Y., Chan, A.H., Judge, L.M., Yoo, J., Huang, M., Nguyen, T.D., Lizarraga, P.P., So, P.-L., and Conklin, B.R. (2014). Isolation of single-base genome-edited human iPS cells without antibiotic selection. Nat. Methods *11*, 291–293. https://doi.org/10.1038/nmeth.2840.

68. HD; iPSC Consortium (2017). Developmental alterations in Huntington's disease neural cells and pharmacological rescue in cells and mice. Nat. Neurosci. *20*, 648–660. https://doi.org/10.1038/nn.4532.

69. Eichel, K., Uenaka, T., Belapurkar, V., Lu, R., Cheng, S., Pak, J.S., Taylor, C.A., Südhof, T.C., Malenka, R., Wernig, M., et al. (2022). Endocytosis in the axon initial segment maintains neuronal polarity. Nature *609*, 128–135. https://doi.org/10.1038/s41586-022-05074-5.

70. Tristan, C.A., Hong, H., Jethmalani, Y., Chen, Y., Weber, C., Chu, P.-H., Ryu, S., Jovanovic, V.M., Hur, I., Voss, T.C., et al. (2023). Efficient and safe single-cell cloning of human pluripotent stem cells using the CEPT cocktail. Nat. Protoc. *18*, 58–80. https://doi.org/10.1038/s41596-022-00753-z.

## STAR★METHODS

### KEY RESOURCES TABLE

| REAGENT or RESOURCE | SOURCE | IDENTIFIER |
|---|---|---|
| Antibodies | | |
| Anti-Cas9 antibody | Takara | Cat#632607; RRID: AB_3251495 |
| Anti-MAP2 antibody | Sigma | Cat#M4403; RRID: AB_477193 |
| Anti-Cas9 (7A9-3A3) antibody (Figure S3) | Cell Signaling Technology | Cat#14697S; RRID:AB_2750916 |
| Anti-HA (C29F4) antibody | Cell Signaling Technology | Cat#3724S; RRID:AB_1549585 |
| Goat anti-Mouse IgG (H+L) Highly Cross-Adsorbed Secondary Antibody, Alexa Fluor Plus 647 | Invitrogen | Cat#A32728; RRID:AB_2633277 |
| Goat anti-Rabbit IgG (H+L) Highly Cross-Adsorbed Secondary Antibody, Alexa Fluor Plus 488 | Invitrogen | Cat#A32731; RRID:AB_2633280 |
| Anti-LMX1 antibody | Sigma-Aldrich | Cat#AB10533; RRID: AB_3669120 |
| Anti-TH antibody | Pel-Freez | Cat#P40101-0; RRID: AB_461064 |
| Anti-FOXA2 antibody | R and D Systems | Cat#AF2400; RRID: AB_2294104 |
| Chemicals, peptides, and recombinant proteins | | |
| mTeSR1 medium | Stem Cell Technologies | Cat#85850 |
| Accutase | Innovative Cell Technologies | Cat#AT-104 |
| StemFlex medium | Thermo Fisher | Cat#A3349401 |
| Y-27632 | Axon Medchem | Cat#Axon 1683 |
| DMEM/F-12 | Thermo Fisher | Cat#11320-082 |
| Neurobasal medium | Thermo Fisher | Cat#21-103-049 |
| Matrigel | Corning | Cat#356234 |
| B27 supplement | Thermo Fisher | Cat#17504044 |
| N2 supplement | Thermo Fisher | Cat#17502048 |
| Glutamax | Thermo Fisher | Cat#11360-070 |
| Lipofectamine Stem | Thermo Fisher | Cat#STEM00003 |
| Puromycin | Sigma | Cat#P8833 |
| Doxycycline | Sigma | Cat#D9891 |
| Insulin | Sigma | Cat#I6634 |
| MEM Non-Essential Amino Acids Solution | Thermo Fisher | Cat#11140076 |
| Chroman I | MedChem Express | Cat#HY-15392 |
| Papain Dissociation System | Worthington | Cat#LK003150 |
| Experimental models: Cell lines | | |
| Human embryonic kidney (HEK) 293T/17 cells | ATCC | ATCC Cat# CRL-11268; RRID: CVCL_0063 |
| KOLF2.1J | The Jackson Laboratory | hPSCreg: WTSIi018-B-12 |
| Human embryonic stem cells (ESCs) line H1 | WiCell Research Institute, Inc. | WiCell Cat# wa01-cgmp-material; RRID: CVCL_9771 |
| Human embryonic stem cells (ESCs) line HS980 | Karolinska Institute, Stockholm, Sweden | HS980; RRID: CVCL_2Z88 |
| BIONi010C | European Bank for Induced pluripotent Stem Cells (EBiSC) | BIONi010-C; RRID:CVCL_1E68 |
| CS83iCTR33n1 | Cedars-Sinai Biomanufacturing Center | CS83iCTR33-n1; RRID:CVCL_IW28 |
| WTC11 | Coriell Catalog | Coriell Cat#GM25256; RRID:CVCL_Y803 |
| Experimental models: Organisms/strains | | |
| Mouse CD1 | Charles River | strain code 022 |

(*Continued on next page*)

| *Continued* | | |
|---|---|---|
| REAGENT or RESOURCE | SOURCE | IDENTIFIER |
| Oligonucleotides | | |
| qPCR primers | This paper | see Table S2 for sequences and information |
| Recombinant DNA | | |
| TK4-NLS-EGFP | This paper | Addgene plasmid #239046 |
| TK4-mScarlet | This paper | N/A |
| TK4-zim3-dCas9 | This paper | N/A |
| SH4-1 targeting vector | This paper | N/A |
| SH4-2 targeting vector | This paper | N/A |
| SH7 targeting vector | This paper | N/A |
| SH7-flip targeting vector | This paper | N/A |
| CLYBL targeting vector | This paper | N/A |
| FUW-TetO-Ngn2- P2A-puromycin | Zhang et al.[63] | Addgene plasmid #52047 |
| FUW-rtTA | Hockemeyer et al.[64] | Addgene plasmid #20342 |
| pRSV-rev | Dull et al.[65] | Addgene plasmid #12253 |
| pMDLg/ pRRE | Dull et al.[65] | Addgene plasmid #12251 |
| pMD2.G | Trono Lab Packaging and Envelope Plasmids (unpublished) | Addgene plasmid #12259 |
| Software and algorithms | | |
| GraphPad Prism 10 | https://www.graphpad.com | RRID:SCR_002798 |
| Fiji | http://www.imagej.net/Fiji | RRID:SCR_002285 |
| SnapGene | https://www.snapgene.com/ | RRID:SCR_015052 |
| FlowJo v10 | https://www.flowjo.com/ | RRID:SCR_008520 |
| Biorender | https://www.biorender.com/ | N/A |

## EXPERIMENTAL MODEL AND STUDY PARTICIPANT DETAILS

### Cell lines

All human iPSCs and ESCs used in this study were previously generated and reported to be derived from material obtained under informed consent and appropriate ethical approvals.

### iPS Cell Culture and Generation of Polyclonal Lines Using PiggyBac Vector (Wernig lab)

Male human embryonic stem cells (ESCs) line H1 and KOLF2.1J iPS cell line, were cultured on Matrigel-coated plates in StemFlex media. For transfection, $1.5 \times 10^6$ iPSCs per well were seeded in a 6-well plate with 1.5 mL of E8 media supplemented with Y-27632 and incubated for 2 hours. The transfection mix was prepared by combining 1333 ng of the TK4 vector with 666 ng of transposase in 250 μL OPTI-MEM, along with 5 μL of Lipofectamine STEM reagent. This mixture was incubated at room temperature for 30 minutes. After the 2-hour incubation, wells were washed with DPBS, followed by the addition of 1.5 mL of E8 media with Y-27632. The transfection mix was then added dropwise to the cells. The following day, the medium was replaced with StemFlex media containing Y-27632. Two days post-transfection, Y-27632 was removed, and three days post-transfection, puromycin selection (2 μg/mL) was started. The cells were passaged at least twice in puromycin-containing media.

### iPS cell culture and nucleofections for gene targeting (Skarnes lab)

KOLF2.1J cells[29] were cultured on Synthemax or vitronectin-coated plates in complete StemFlex media and nucleofected with Cas9 RNP as described previously.[66] TK4 construct with 400 bp homology arms was integrated into 3 safe harbor loci (SH4-1, 4-2 and 7) and 1,000 bp homology arms was integrated into CLYBL locus by CRISPR genome editing. Plasmid DNA donors were ethanol precipitated and resuspended in P3 primary buffer prior to use. Each nucleofection contained two micrograms of plasmid DNA donor, 20 ug HiFi Cas9 recombinant protein (IDT) and 16ug guide RNA (Synthego) in a volume of 0.1 ml Primary buffer 3 plus Supplement (Lonza). Nucleofected cells were plated in Stem Flex media containing ROCK inhibitor (1X Revitacell; Invitrogen). After 48 hours, the media was replaced with Stem Flex containing 0.5 microgram/ml puromycin and changed every two days until colonies formed. The colonies were pooled and cultured in presence of puromycin for two passages prior to single cell cloning. Four hundred single cells were plated on a vitronectin-coated 10cm dish in Stem Flex media containing CloneR2 (Stem Cell Technologies) and the media was changed every two days until colonies appeared. Individual colonies were picked into replicate vitronectin-coated 96-well plates, expanded and archived or lysed for genotyping as described.[66]

### Human stem cells (Kampmann lab)

Human iPSCs in the male WTC11 background[67] were cultured in StemFlex Medium on BioLite Cell Culture Treated Dishes (Thermo Fisher Scientific; assorted Cat. No.) coated with Growth Factor Reduced, phenol red-Free, LDEV-Free Matrigel Basement Membrane Matrix (Corning; cat. No. 356231) diluted 1:100 in Knockout DMEM (GIBCO/Thermo Fisher Scientific; cat. No. 10829-018). Routine passaging was performed as described (Tian et al. Neuron 2019). Studies with human iPSCs at UCSF were approved by the The Human Gamete, Embryo and Stem Cell Research (GESCR) Committee. Informed consent was obtained from the human subjects when the WTC11[67] lines were originally derived.

### Stem cell culture (Arenas lab)

Kolf2.1J human induced pluripotent stem cells and HS980 human embryonic stem cells were maintained undifferentiated in E8Flex media on laminin 521 (Biolamina)-coated plates, 20,000 cells/cm$^2$ and passaged with ReLeSr (StemCell Technologies) or TrypLE select (Thermo Fisher), respectively. Kolf2.1J and HS980 stem cells were transfected with the TK4 PiggyBac vector and transposase plasmids at a ratio of 3:1 using nucleofection P3 primary cell kit (Amaxa 4D-nucleofector Lonza), 3 μg total DNA to 800,000 cells. Transfected cells were selected using 2 μg/ml Puromycin and stable polyclonal batches were cryopreserved.

### iPSC Culture (Kronenberg-Versteeg lab)

Human induced pluripotent stem cells (iPSC) lines BIONi010-C, (European Bank for Induced Pluripotent Stem Cells, UK), and KOLF2.1J (Jackson Laboratories, USA) were maintained on Geltrex (ThermoFisher Scientific)-coated 6-well plates (Corning) in mTeSR Plus (mTeSR+, Stemcell Technologies) media until reaching ∼80 % confluency and split using ReLeSR (Stemcell Technology) during maintenance and prior further processing. For the first 24 h after splitting, 10 μM Rock Inhibitor Y27632 (Stemcell Technologies) was added to the medium to enhance cell survival. iPSCs were cultured at 37 °C, 5 % CO2 and 100 % humidity with media changes 24 h after splitting and subsequently every other day.

### Stem Cell Culture (Thompson lab)

Human iPSC lines KOLF2.1J, and CS83iCTR33n1[68] were maintained on hESC-qualified Matrigel (Corning) in mTeSR+ medium and passaged with ReLeSR (both Stemcell Technologies). For transfection, cells were dissociated with Accutase (Invitrogen) and 200,000 cells transfected with TK4 PiggyBac vector and K13-Transposase PiggyBac plasmids at a donor:transposase ratio of 3:1 (5.33μg total DNA) using Nucleofector Solution Kit 2 (Lonza) with the Nucleofector 2b device, program B-016. Cells were allowed to recover in mTeSR+ medium supplemented with CloneR (Stemcell Technologies) and transitioned to mTeSR+ containing 1μg/ml puromycin 48hr post transfection.

## METHOD DETAILS

### Lentiviral generation

Lentiviruses were produced in HEK293T cells (ATCC) as described previously.[69] The expression vector (Ngn2-T2A-puromycin[63] and rtTA[64]) and three helper plasmids (pRSV–REV,[65] pMDLg/pRRE[65] and VSV-G) were co-transfected with polyethylenimine. Lentiviral particles were ultra-centrifuged, re-suspended in DMEM, snap-frozen, and stored at −80°C.

### Generation of Ngn2-iN cells (Wernig lab)

iPSCs were differentiated with slight modifications to a previously described protocol.[63,69]

KOLF2.1J-Ngn2 cells were plated as dissociated cells in a 24-well plate (10–20 × 10$^3$ cells) or 384-well plate (1–2 × 10$^3$ cells) on day 0. From day 0 of differentiation, we discontinued puromycin in the media of TK4 vector-expressing cells to assess silencing of the transgenes. H1 cells without Ngn2 cassette were plated with lentiviruses containing expression constructs of Ngn2-T2A-puromycin and rtTA. On day 1, the culture medium was replaced with N3 media (composed of DMEM/F12 [Thermo Fisher], N2 supplement [Thermo Fisher], and MEM Non-Essential Amino Acids [Thermo Fisher], supplemented with insulin [Sigma]), containing doxycycline (2 μg/mL, Sigma) to induce Ngn2 expression. On days 4 and 5, AraC (4 μM, Sigma) was added to eliminate dividing cells. On day 6, passage 3 mouse glial cells were added on top of the neurons (3 × 10$^4$ mouse glial cells per well of a 24-well plate, and 1.5 × 10$^3$ cells per well in a 384-well plate), re-suspended in Neurobasal media (Thermo Fisher) supplemented with B27 (Thermo Fisher), Glutamax (Thermo Fisher), and 5% fetal bovine serum (FBS, GE Healthcare). On day 7, the medium was changed to Neurobasal media with B27, Glutamax, 2% FBS, and AraC (4 μM). Approximately 30% of the media was exchanged every 3-4 days. All animal studies were approved by the Administrative Panel on Laboratory Animal Care (APLAC, Stanford University), and CD1 mice (Charles River) were used in this study.

### Flow cytometry analysis (all participating labs)

iPS cells containing each PiggyBac vector were prepared in 24-well plates as described above. At each time point, the cells were dissociated using 250 μL of Accutase, resuspended in FACS buffer (R&D) supplemented with Y-27632, and filtered through a 70 μm strainer for flow cytometry analysis using a FACSAria instrument. After doublet discrimination, the median fluorescence intensity was measured using FlowJo software.

### Confocal microscopy analysis (Wernig lab)

iPS cells containing each PiggyBac vector were prepared in 384-well plates as described above. At each time point, images were captured using a Nikon Spinning Disk confocal microscope (Nikon) or LSM980 (Zeiss) with a 20x objective lens, utilizing 4-tile imaging. GFP-positive areas were identified, and samples that were too sparse or too dense were excluded based on the area count. EGFP intensity within the positive areas was quantified using ImageJ software.

### Immunostaining and measurement of dCas9 intensity (Wernig lab)

Coverslips were fixed with 4% paraformaldehyde (PFA) for 10 minutes at room temperature (RT) at each time point. All coverslips from day 0 to day 48 in the same batch were stained simultaneously. After washing with PBS, cells were permeabilized with 0.2% Triton X-100 in PBS for 8 minutes, followed by incubation with blocking buffer (5% BSA in PBS with 0.1% Triton X-100) for 1 hour at RT. Cells were then incubated overnight at 4 °C with primary antibodies diluted in blocking buffer: Cas9 (Takara, 632607; 1:200) and MAP2 (Sigma, M4403; 1:500). The next day, after PBS washes, cells were incubated with secondary antibodies diluted in blocking buffer for 1 hour at RT. Ccoverslips were then washed with PBS and mounted using DAPI Fluoromount-G® (SouthernBiotech, #0100-20). Images were acquired using a ZEISS LSM980 confocal microscope with a 20× objective. For each condition, 4–5 fields were imaged per batch. Cas9 intensity was measured in ImageJ. Briefly, the ROI for the MAP2-positive area was applied to the DAPI channel to detect neuronal nuclei. This ROI was then applied to the dCas9 channel to measure dCas9 intensity in neuronal nuclei. Total intensity was normalized to the number of neuronal nuclei to calculate intensity per cell. The ImageJ script is available upon request.

### RNA extraction and qRT-PCR (*Wernig lab*)

Adherent cells were lysed in TRIzol (Thermo Fisher Scientific), and total RNA was purified using the RNA Clean & Concentrator-5 kit (Zymo Research). cDNA was synthesized using SuperScript III reverse transcriptase (Thermo Fisher Scientific). Quantitative real-time PCR was performed using SYBR Green Universal Master Mix (Thermo Fisher Scientific) with primers listed in Table S2 on a QuantStudio 7 real-time PCR system (Thermo Fisher Scientific). Relative gene expression levels were determined using standard curve–based quantification and normalized to internal reference genes.

### Genotyping (Skarnes lab)

PCR amplification and Sanger sequencing was performed from diluted crude whole cell lysates.[66] Briefly, lysates were diluted 1:10 and 2ul was used in a 20 microliter reaction containing PrimeSTAR GXL polymerase (Takara) and 0.25 micromolar PCR primer pairs spanning the 5' and 3' homology arms. Correctly targeted clones were identified by gel electrophoresis and GFP expression was confirmed by FACS. Primers for genotyping are listed on Table S3.

### Ngn2-neuron Differentiation (Kampmann lab)

Human iPSC-derived neurons were pre-differentiated and differentiated as described.[21] Briefly, iPSCs were pre-differentiated in Matrigel-coated plates or dishes in N2 Pre-Differentiation Medium containing the following: KnockOut DMEM/F12 as the base, 1× MEM non-essential amino acids, 1× N2 Supplement (Gibco/Thermo Fisher Scientific, cat. no. 17502-048), 10 ng $ml^{-1}$ of NT-3 (PeproTech, cat. no. 450-03), 10 ng $ml^{-1}$ of BDNF (PeproTech, cat. no. 450-02), 1 μg $ml^{-1}$ of mouse laminin (Thermo Fisher Scientific, cat. no. 23017-015), 10 nM ROCK inhibitor and 2 μg $ml^{-1}$ of doxycycline to induce expression of mNGN2. After 3 d, on the day referred to hereafter as Day 0, pre-differentiated cells were re-plated into BioCoat poly-D-lysine-coated plates or dishes (Corning, assorted cat. no.) in regular neuronal medium containing the following: half DMEM/F12 (Gibco/Thermo Fisher Scientific, cat. no. 11320-033) and half neurobasal-A (Gibco/Thermo Fisher Scientific, cat. no. 10888-022) as the base, 1× MEM non-essential amino acids, 0.5× GlutaMAX Supplement (Gibco/Thermo Fisher Scientific, cat. no. 35050-061), 0.5× N2 Supplement, 0.5× B27 Supplement (Gibco/Thermo Fisher Scientific, cat. no. 17504-044), 10 ng $ml^{-1}$ of NT-3, 10 ng $ml^{-1}$ of BDNF and 1 μg $m^{-1}$ of mouse laminin. Neuronal medium was half-replaced every week. Full protocols are available on protocols.io (dx.doi.org/10.17504/protocols.io.bcrjiv4n).

At each time point, cells were washed with 1mL DPBS and then 200uL accutase was added for 7 minutes. Cells were resuspended in DPBS+rock inhibitor, and strained through a 70um filter and subjected to flow cytometry.

### 6TF-Microglia Differentiation (Kampmann lab)

Microglia were differentiated as in the previous paper.[28] Briefly, iPS cells containing six doxycycline-inducible transcription factors: CEPBA, CEBPB, IRF5, IRF8, MAFB, PU.1 were passaged as a single cell suspension using accutase (Thermo Fisher Scientific A11105-01) onto Matrigel and PDL coated plates. Cells were maintained for 2 days in Essential 8 stem cell maintenance media supplemented with doxycycline and 10 uM Y-27632 (Tocris 1254). On day 2 post passage, media was replaced with Advanced DMEM/F12, 1x Glutamax, 2 ug/mL doxycycline, 100 ng/mL IL-34 (Peprotech 200-34), and 10 ng/mL GM-CSF (Peprotech 300-03). On day 4, media was replaced with Advanced DMEM/F12, 1x Glutamax, 2 ug/mL doxycycline, 100 ng/mL IL-34, 10 ng/mL GM-CSF, 50 ng/mL M-CSF (Peprotech 300-25), and 50 ng/mL TGFB (Peprotech100-21C). Media was replaced on d8, d12, and d15.

On each collection day (d0, d2, d4, d8, d12, d15), microglia were lifted for 10 min at 37C with TrypLE.

### Midbrain Dopaminergic Neuron Differentiation (Arenas lab)

Kolf2.1J and HS980 stem cells were seeded at a density of 200,000 cells/cm2 on Geltrex-(Life Technologies) and Laminin 511-(Biolamina) coated wells and differentiated towards midbrain dopaminergic neurons according to the Arenas Lab protocol in the previous paper.[29] At day 11 and day 16 cells were replated at a density of 500,000 cells/cm2 on 1 μg/mL laminin 511 coated wells (day 11) plus 15 μg/mL poly-L-ornithine (Sigma Aldrich) (day 16).

For Kolf2.1J and HS980 cell lines, parental (wild-type) and TK4 PiggyBac-expressing stem cells were maintained undifferentiated or differentiated to dopaminergic neurons and processed in parallel for FACS analysis of BFP and EGFP at days 0, 7, 14, 21 and 28. Undifferentiated stem cells were maintained in the presence of puromycin selection, whilst differentiating cells were not. Cells were dissociated into single cell suspensions using TrypIE-Select (Thermo Fisher), collected in direct trypsin inhibitor (Thermo Fisher), centrifuged at 300 x g for 5 mins and resuspended at 1,000,000 cells/ ml in FACS buffer (0.5% BSA in PBS). Cells were sorted using a 100 μm nozzle with gating to define single cells (BD Facs Aria II with BD FACSDiva 9.0.1 software). BFP+ and EGFP+ cells were defined as singlet cells with signal above the negative control for each cell line (parental, non-expressing WT stem cells).

### Embryoid body-based Microglia Differentiation (Kronenberg-Versteeg lab)

iPSC-derived microglia (iMic) were generated following Haenseler et al.'s protocol[32] with small modifications. In brief, iPSCs were washed once with PBS (Gibco) and detached using ReLSR for 5–6 minutes. Cells were collected in Wash Buffer (Dulbecco's Modified Eagle's Medium (DMEM)-F12 (Gibco) + 0.1 % BSA Fraction V (Gibco)) and the cell suspension was centrifuged at 300 g (Heraeus Multifuge 3-SR). The supernatant was aspirated, the cells were resuspended to single-cell suspension in Wash Buffer and the cell number was determined using a hemocytometer (Neubauer Zählkammer Improved, Bard).

To generate embryoid bodies (EB) of approximately the same size, 2.5 mil iPSCs per well in 2 ml EB Induction Medium (mTeSR+ + 20 ng/ml SCF (R & D Systems) + 50 ng/ml BMP4 (Miltenyi) + 50 ng/ml VEGF (Miltenyi), supplemented with 10 μM Y27632 (Stem Cell Technologies) for the first 24 hours) were seeded into an AggreWell800 plate of the 24-well format (Stem Cell Technologies), that was prepared with anti-adherence rinsing solution (Stemcell Technologies). The cells were cultivated in the microwell plate to allow the formation of EBs at 37 °C and 5 % CO2 for 5 days with partial (75 %) media changes every day.

After 5 days, the EBs were harvested and equally distributed into 12 wells of 6-well plates in 2 ml of EB Differentiation Media (X-Vivo 15 (Lonza), 2 mM Glutamax (Gibco), 0.55 mM β-mercaptoethanol (Gibco), 100 U/ml/100 μg/ml Penicillin/Streptomycin (ThermoFisher Scientific), 25 ng/ml IL-3 (Miltenyi Biotec), 100 ng/ml M-CSF (Miltenyi Biotec)) per well.

The EBs were kept in EB Differentiation Media at 37 °C and 5 % CO2 with media changes every 7 days.

After 2-3 weeks of cultivation, non-adherent microglial precursor cells (pre-iMic) started emerging and were harvested from EB cultures by collecting the supernatant cell culture medium.

### Monolayer-based Microglia Differentiation (Kronenberg-Versteeg lab)

Additionally, iPSCs were differentiated to microglia using a monolayer-based protocol established by Takata et al.[33] In brief, iPSCs were plated in clumps at 7,000 cells/cm2 onto GTX-coated 12-well plates (Corning) in mTeSR+ supplemented with 10 μM Rock-Inhibitor. After 24 hours, medium was changed to Supplemented Stempro-34 SFM (Gibco) medium (+ 2 mM Glutamax (Gibco), 5 μM Ascorbic Acid (Sigma-Aldrich), 150 μg/ml Transferrin (Roche), 0.45 mM Monothioglycerol (Sigma-Aldrich), 100U/ml/100μg/ml Penicillin/Streptomycin (Gibco)) for the remainder of cultivation period, with medium changes every 2 days. On Day 0, medium was supplemented with 5 ng/ml BMP4 (Miltenyi), 50 ng/ml VEGF (Peptrotech) and 2 μM CHIR99021 (Miltenyi) and cells were transferred to hypoxia conditions for the next 8 days (37 °C, 5 % CO2, 5 % O2). On Day 2, medium was supplemented with 5 ng/ml BMP4, 50 ng/ml VEGF and 20 ng/ml bFGF (Miltenyi). On Day 4, medium contained 15 ng/ml VEGF, 5 ng/ml bFGF. From Day 6 onwards, floating precursor cells started to emerge, which were collected with the supernatant, centrifuged at 300 g for 5 min and then re-administered to the culture wells. Media composition for Day 6-10: Supplemented Stempro-34 + 10 ng/ml VEGF, 10 ng/ml bFGF, 10 ng/ml IL6 (Miltenyi), 20 ng/ml IL3 (Miltenyi), 30 ng/ml DKK1 (Miltenyi), 50 ng/ml SCF (R&D Systems). On Day 8 cells were transferred to normoxic incubator conditions (37 °C, 5 % CO2, atmospheric O2). For Day 12 and 14, medium was supplemented with 10 ng/ml bFGF, 10 ng/ml IL6, 20 ng/ml IL3 and 50 ng/ml SCF. For final differentiation, the medium was supplemented with 50 ng/ml CSF1 (Miltenyi) on Days 16-20, before pre-iMics were harvested and differentiated as described below.

### Final Microglia Differentiation and Maturation (Kronenberg-Versteeg lab)

For both protocols, pre-iMics were harvested from the supernatant cell culture medium by collecting the medium and centrifuging at 300 g for 5 minutes. The supernatant was aspirated, and cells were counted using a hemocytometer.

Pre-iMics were seeded at a density of 20,000 cells/cm2 on TC-treated cell culture plates (12-well, Corning) and differentiated to microglia in microglia differentiation medium (50 % Neurobasal Medium (Gibco), 50 % DMEM-F12 (Gibco), 1x B27 Supplement with Vitamin A (Gibco), 2 mM Glutamax (Gibco), 0.1 mM β-mercaptoethanol (Gibco), 100 ng/ml IL-34 (Miltenyi Biotec), 20 ng/ml M-CSF (Miltenyi Biotec) for up to 7 days with 3 medium changes per week.

To assess, signal intensities of BFP and GFP, cells were used for FACS analysis two times per week for the duration of the differntiation process.

At each timepoint, one well of the monolayer-based differentiation protocol and ca. 5 EBs were sacrificed and analyzed in FACS.

Cells growing in monolayer (iPSCs, monolayer-based differentiation protocol, iMics) were washed once with PBS and incubated with Accutase (Gibco) for 5-6 minutes at 37 °C, washed with Wash Buffer, collected and centrifuged at 300 g for 5 min and

resuspended in FACS Buffer (PBS, 0.1 % BSA Fraction V (Gibco)). EBs were collected, washed once with PBS, incubated with Accutase for 15-20 minutes at 37 °C with intermediate vortexing and afterwards processed as cells grown in monolayer. Free-floating pre-iMics were collected from the supernatant as described above and used for FACS analysis on the day of plating pre-iMics. Cells were analyzed using a Sony SH800 cell sorter.

### Striatal Neuron Differentiation (Thompson lab)

Neuronal differentiation was performed once iPSC colonies reached 60–70% confluency as previously described.[34] Differentiation was initiated (Day 0) by washing iPSC colonies with phosphate-buffered saline pH 7.4 (PBS – Gibco) and switching to SLI medium (Advanced DMEM/F12 (1:1) supplemented with 2 mM GlutamaxTM (Gibco), 2% B27 without vitamin A (Life Technologies), 10 μM SB431542, 1 μM LDN 193189 (both Stem Cell Technologies), 1.5 μM IWR1 (Tocris)) with daily medium changes. Four days later, cells were pretreated with 50nM Chroman 1 (MedChem Express), washed with PBS, and passaged 1:2 with StemPro Accutase (Invitrogen) for 5 minutes at 37 °C. Cells were replated onto plates coated with hESC qualified matrigel (1 h at 37 °C) in SLI medium containing CEPT cocktail (50 nM Chroman 1, 5 μM emricasan (Selleck Chemicals), Polyamine Supplement (1:1000, Sigma-Aldrich), 0.7 μM trans-ISRIB (R&D Systems)) for 1 day after plating and continued daily feeding with SLI medim. At day 8, cells were passaged 1:2 as above and replated in LIA medium (Advanced DMEM/F12 (1:1) supplemented with 2 mM GlutamaxTM, 2% B27 without vitamin A, 0.2 μM LDN 193189, 1.5 μM IWR1, 20 ng/ml Activin A (Peprotech)) with CEPT cocktail for 1 day after plating and daily feeding was continued through day 16. At day 16, cells were pretreated with 50nM Chroman 1, dissociated with Accutase, and plated in 6-well Nunclon plates coated with PDL and hESC Matrigel at $1 \times 10^6$ per well in SCM1 medium (Advanced DMEM/F12 (1:1) supplemented with 2 mM GlutamaxTM, 2% B27 (Invitrogen), 10 μM DAPT, 10 μM Forskolin, 300 μM GABA, 3 μM CHIR 99021, 2 μM PD 0332991 (all Tocris), 1.8 mM CaCl2, 200 μM ascorbic acid (Sigma-Aldrich), 10 ng/ml BDNF (Peprotech)). Medium was 50% changed every 2-3 days. On day 23, medium was fully changed to SCM2 medium (Advanced DMEM/F12 (1:1): Neurobasal A (Gibco) (50:50) supplemented with 2 mM GlutamaxTM), 2% B27, 1.8 mM CaCl2, 3 μM CHIR 99021, 2 μM PD 0332991, 200 μM ascorbic acid, 10 ng/ml BDNF) and 50% medium changes performed every 2–3 days. Cells were considered mature at day 37.

### Hypothalamic neuron differentiation (Merkle lab)

KOLF2.1J hiPSCs were maintained in StemFlex iPSC medium (Thermo Fisher Scientific) on 6-well plates coated with Geltrex™ (Thermo Fisher Scientific). Cells were kept in humidified incubators at 37°C and 5% CO2, fed daily with full media changes, and passaged at 60-70% confluence with 0.5 mM EDTA for 5 min at 37°C. Upon removal of EDTA, cells were resuspended and re-plated in StemFlex medium containing 10 μM Y-27632 onto Geltrex™ - coated plates at split ratios of 1:10 – 1:12.

KOLF2.1J hiPSCs were dissociated into single cell suspension using StemPro™ Accutase™ Cell Dissociation Reagent (Thermo Fisher Scientific) for 5 min at 37°C. Cells were then washed and collected with StemFlex + 10 μM Y-27632 (DNSK International) before being centrifuged at 300xg for 4 mins. The supernatant was removed, and the cell pellet was resuspended in StemFlex + 10 μM Y-27632. A cell count was then performed. KOLF2.1J hiPSCs were then seeded at 100k/$cm^2$ in StemFlex + 10 μM Y-27632 in 12-well plates on Day -1. Differentiation was carried out according as previously described.[35] On Day 0, the medium was changed to the differentiation medium of N2B27 containing 100 nM LDN-193189 (DNSK International), 10 μM SB431542 (DNSK International), and 2 μM XAV939 (DNSK International). Medium was changed every other day as described in the tables below until Day 13, to generate hypothalamic neural progenitor cells (NPCs). At Day 13, NPCs were dissociated into single cell suspension using StemPro™ Accutase™ Cell Dissociation Reagent and seeded in N2B27 medium + 10uM Y-27632 into 12-well plates at $3x10^5$ cells per $cm^2$. On Day 14, the medium was changed to Synaptojuice 1 (SJ1) maturation medium supplemented with 10 ng/ml brain-derived neurotrophic factor, BDNF (PeproTech). The cells were maintained in SJ1 + 10 ng/ml BDNF for a week with medium changes every other day. On Day 21, the medium was switched to Synaptojuice 2 (SJ2) medium with 10 ng/ml BDNF and maintained in this medium with media changes every second day until Day 30 to generate functional hypothalamic neurons. At different time points along the differentiation timeline (Day -1 to Day 28), cells were dissociated into single cell suspensions in FACS buffer made up of DPBS (-/-) (Thermo Fisher Scientific) with 0.2% BSA (Sigma-Aldrich), 1 mM EDTA (Thermo Fisher Scientific) and 25 mM HEPES (Thermo Fisher Scientific) before being run through a BD Fortessa Cell Analyser. 3 technical replicates per sample, containing 1 million cells each were run in the cell analyser at each time point. 10,000 events were captured per technical replicate. In the FSC/SSC plot, cells were selected using a gate high for FSC and SSC to exclude debris. Separate histogram plots of BFP (violet laser 450/50) and GFP (blue laser 530/30) were generated from the gated cell population to show the cells positive for each fluorophore.

### Cortical neuron differentiation (Schüle lab)

Human induced pluripotent stem cell (iPSC) reference line KOLF2.1J and line SUSL25 carrying a LRRK2 G2019S mutation associated with Parkinson's disease were cultured in StemFlex media (Thermo Fisher Scientific, A3349401) on Matrigel substrate (Thermo Fisher Scientific, CB-40230) diluted in KnockOut DMEM (1:90, Thermo Fisher Scientific, 10829018). Cells were routinely passaged with ReLeSR (StemCell Technologies, 05872) at 80% confluence with supplementation of media with 1 uM of ROCK inhibitor Thiazovivin (ReproCell, 04-0017). Prior to transfection and differentiation, both iPSC lines were passaged at least twice under these conditions and synchronized to be transfected on the same day. Both iPSC lines were confirmed to be healthy and free of spontaneous differentiation as evidenced by microscopy observations of tightly packed colonies with distinctive edges, high nucleus-to-cytoplasm ratios, and prominent nucleoli.

On the day of transfection, both iPSC lines were dissociated into single cells with Accutase (Fisher Scientific, NC9464543), counted, and plated in a Matrigel-coated 6-well plate at a cell density 150,000 cells/cm2 in 1.5 ml of mTesR1 (STEMCELL Technologies, 85850) media supplemented with 1X CEPT (Chroman 1 (MedChem Express, HY-15392); Emricasan (Selleck Chemicals, S7775); Polyamine Supplement (Sigma-Aldrich, P8483-5ML); Trans-ISRIB (Tocris, 5284)). The use of CEPT in cell culture was previously described.[70] Cells were incubated for 2 hours at 37°C with 5% CO2. After 2 hours, the cells were washed with PBS without Ca2+ and Mg2+ (Fisher Scientific, 70-011-044) and the media was changed to fresh 1.5 ml of mTesR1 supplemented with 1X CEPT. The transfection mix was added dropwise to both cell lines and evenly distributed in the media by swirling the plate and performing quick side-to-side shaking of the plate. Cells were incubated for 24 hours at 37°C with 5% CO2. After 24 hours post-transfection, the media was switched to 2 ml StemFlex with 1X CEPT. After 48 hours post-transfection, the media was changed to 2 ml StemFlex to allow cells to recover. After 72 hours post-transfection, the media was changed to 2 ml StemFlex supplemented with 2 ug/ml puromycin (Invivogen, ant-pr-1). Cells were cultured in StemFlex with Puromycin for at least two passages before differentiation, excluding the addition of Puromycin on the day of passaging and supplementing media with 1X CEPT. After confirming stable expression of GFP by FACS, cells were taken off Puromycin and maintained in StemFlex.

For differentiation of iPSCs to neuronal progenitor cells (NPCs) on day -1, both iPSC lines were dissociated into single cells with Accutase, counted, and plated in a Matrigel-coated 6-well plate at a cell density 350,000 cells/cm2 in 2 ml of media mix that consisted of 50% StemFlex and 50% Neuronal Maintenance Media (NMM) base (Neurobasal™ Medium (serves as base, Thermo Fisher Scientific, 21103049); DMEM/F12, GlutaMAX Supplement (serves as base, Thermo Fisher Scientific, 10-565-018); Beta-Mercaptoethanol (0.1 mM, Thermo Fisher Scientific, 21985023); Penicillin-Streptomycin (1X, Thermo Fisher Scientific, 15140-122); NEAA (1X, Thermo Fisher Scientific, 11140050); GlutaMAX (1X, Thermo Fisher Scientific, 35050-061); Insulin (0.22 uM, added after filtering, Sigma-Aldrich, I9278); N2 supplement (0.5X, added fresh in weekly aliquots, Thermo Fisher Scientific, 17502-048); B27 without Vitamin A (0.5X, added fresh in weekly aliquots, Thermo Fisher Scientific, 12587010)) without the addition of insulin, N2, and B27 but with supplementation of 1X CEPT. Cells were incubated for 24 hours at 37°C with 5% CO2. After 24 hours of incubation on day 0, the media in both cell lines was changed to 4 ml/well of complete NMM (with insulin, N2, and B27) supplemented with 500 nM LDN (Peprotech, 1066208) and 10 uM SB 431542 (Peprotech, 3014193). Cells were incubated for 48 hours at 37°C with 5% CO2. Media changes to 4 ml/well of NMM with LDN and SB 431542 occurred every other day on days 2, 4, and 6. On day 7, media was changed to 3 ml/well of NMM supplemented with LDN and SB 431542. The first week of differentiation of iPSCs to cortical neurons is a sensitive period when some cell lines may experience cell death and complete detachment due to starvation because of their proliferation properties. Therefore, seeding density and feeding volumes and schedule may need to be adjusted, e.g., decrease cell density and/or increase volume of media and frequency of feeding.

On days 8, 9 and 10, media was changed daily to NMM supplemented with 500 nM LDN only. On day 11, media was changed to 50% complete NMM and 50% complete N2B27 media (Neurobasal™ Medium (serves as base, Thermo Fisher Scientific, 21103049); Penicillin-Streptomycin (1X, Thermo Fisher Scientific, 15140-122); NEAA (1X, Thermo Fisher Scientific, 11140050); GlutaMAX (1X, Thermo Fisher Scientific, 35050-061); N2 supplement (0.5X, added after filtering, Thermo Fisher Scientific, 17502-048); B27 without Vitamin A (0.5X, added after filtering, Thermo Fisher Scientific, 12587010)) supplemented with 500 nM LDN. On days 12, 13, and 14, the media was changed daily to 3 ml/well of complete N2B27 supplemented with 500 nM LDN. On days 15 and 16, the media was changed daily to 3 ml/well of complete N2B27 supplemented with 500 nM LDN and 1 uM CHIR (Peprotech, 2520691). On days 17, 18, and 19, the media was changed daily to 3 ml/well of complete N2B27 supplemented with 1 uM CHIR. On day 20, the media was changed to 3 ml/well of complete N2B27 supplemented with 1 uM CHIR and 1X CEPT.

Double-coated PDL/mouse laminin 12-well plate wells were prepared 24 hours in advance before detaching and replating NPCs for maturation into cortical neurons on day 20. Wells were coated with 500 ul/well of Poly-D-Lysine (PDL, Thermo Fisher Scientific, A3890401) and incubated at room temperature for 1 hour. After 1 hour of incubation, PDL was aspirated, and wells were thoroughly washed with sterile water 3 times. Wells were further coated overnight with 600 ul/well of mouse laminin (SouthernBiotech, 1415-01) diluted in PBS with Ca2+ and Mg2+ (Fisher Scientific, 14-040-133) to 15 ug/ml. The plate was parafilmed and stored at 4°C overnight and then incubated at 37°C for 1 hour before use.

On day 21, NPCs were dissociated into single cells with Accutase, counted, and plated in a 12-well plate coated with PDL/mouse laminin at a cell density 285,000 cells/cm2 in 1 ml of media mix that consisted of 50% complete N2B27 and 50% of Terminal Differentiation (TD) media (Neurobasal A Medium (serves as base, Thermo Fisher Scientific, 12349015); Penicillin-Streptomycin (1X, Thermo Fisher Scientific, 15140-122); NEAA (1X, Thermo Fisher Scientific, 11140050); GlutaMAX (1X, Thermo Fisher Scientific, 35050-061); B27 without Vitamin A (1X, added after filtering, Thermo Fisher Scientific, 12587010); DAPT (10 uM, added after filtering, Peprotech, 2634); L-Ascorbic Acid (0.2 mM, added after filtering, Peprotech, 5088177); db-cAMP (0.5 mM, added after filtering, Peprotech, 1698950); BDNF (10 ng/ml, added fresh before media change, Peprotech, 450-02); GDNF (10 ng/ml, added fresh before media change, Peprotech, 450-10) without the addition of BDNF and GDNF but supplemented with 1X CEPT. Cells were incubated for 24 hours at 37°C with 5% CO2. After 24 hours of incubation on day 22, a half-media change was performed by aspirating 500 ul of media and adding 500 ul of fresh and complete TD media. Half-changes of complete TD media were performed every other day on days 24, 26, 28, and 30 until mature cortical neurons were prepared for the final analysis on day 32. Cortical neurons can be further kept in culture with half-media changes of TD media twice a week, e.g., on Mondays and Fridays until ready for downstream applications.

### Flow cytometry analysis (Ward lab)

Ngn2-iNeurons were matured in 12-well plates for 14 days prior to dissociation with Papain Dissociation System (Worthington, cat#LK003150). Working reagents were reconstituted according to the manufacturer's recommendation with some modification. The final trituration media (TM) used for dissociation contained a final concentration of 0.05% DNase and 50nM Chroman-I (MedChem Express, Cat#HY-15392) in neural maturation media (NMM). Cells were washed with 500µL 0.5mM EDTA and incubated in 250µL of papain solution for 15min at 37C. Papain solution was then gently removed, without disrupting cell monolayer and replaced with 250µL TM. Cells were triturated until no visible clumps remained, then transferred to an eppendorf tube with 250µL PBS. Cells were centrifuged at 500 x g for 5 min, and supernatant removed. The cell pellet was resuspended in 200µL of papain inhibitor, incubated for 5min at room temp and centrifuged at 500 x g for 5 min. Supernatant was removed and the final cell pellet was resuspended in 250µL 4% paraformaldehyde (PFA) prepared in PBS and fixed by incubation for 10min at room temp. After fixation, cells were centrifuged at 500 x g for 5 min, and fixative was removed. To wash, the cell pellet was resuspended in 500µL of PBS to remove residual PFA and then centrifuged at 500 x g for 5 min. Washing was performed a total of 3 times.

For immunostaining, permeabilization/blocking buffer was prepared fresh using 0.2% saponin; 1.5% BSA; in 1xPBS. Primary antibody dilutions were prepared at 1:25 dilution for mouse anti-Cas9 primary (Cell Signaling Technology, Cat#14697S) and 1:1000 dilution for rabbit anti-HA (Cell Signaling Technology, Cat#A32731). Cell pellets were incubated in 100uL of permeabilization buffer with or without primary antibodies for 16hr at 4 degC. To wash, the cell pellet was resuspended in 500µL of ice-cold PBS and then centrifuged at 500 x g for 10 min at 4 degC. Washing was performed a total of 3 times. Secondary antibody solution was prepared using Goat anti-Mouse IgG (H+L) Highly Cross-Adsorbed Secondary Antibody, Alexa Fluor Plus 647 (Cat No. A32728) and Goat anti-Rabbit IgG (H+L) Highly Cross-Adsorbed Secondary Antibody, Alexa Fluor Plus 488 (Cat no: A32731) at 1:500 dilutions in PB. Cell pellets were incubated at room temperature for 1hr. Cells were then centrifuged at 500 x g for 10 min at 4 degC. Supernatant was removed and cell pellets were washed with ice-cold PBS and centrifuged at 500 x g for 10 min at 4 degC for a total of 3 times prior to sorting with BD FACS Symphony A1.

## QUANTIFICATION AND STATISTICAL ANALYSIS

All statistical details for each experiment are provided in the figure legends. Briefly, data are presented as mean ± standard deviation (SD), and "n" denotes the number of independent biological replicates. Statistical analyses and graphical representations were performed using GraphPad Prism (version 10). One-way or two-way ANOVA followed by Tukey's, Dunnett's, or Šídák's multiple-comparison tests were used for comparisons among multiple groups. Statistical significance was indicated by exact p values or as follows: *$P < 0.05$, **$P < 0.01$, ***$P < 0.001$, and ****$P < 0.0001$.